

Majorana CP-violating phases in neutrino-antineutrino oscillations and other lepton-number-violating processes

Zhi-zhong Xing * Ye-Ling Zhou †

Institute of High Energy Physics, Chinese Academy of Sciences, P.O. Box 918, Beijing 100049, China
Theoretical Physics Center for Science Facilities, Chinese Academy of Sciences, Beijing 100049, China

Abstract

If the massive neutrinos are identified to be the Majorana particles via a convincing measurement of the neutrinoless double beta ($0\nu\beta\beta$) decay, how to determine the Majorana CP-violating phases in the 3×3 lepton flavor mixing matrix U will become a desirable experimental question. The answer to this question is to explore all the possible lepton-number-violating (LNV) processes in which the Majorana phases really matter. In this paper we carry out a systematic study of CP violation in neutrino-antineutrino oscillations, whose CP-conserving parts involve six independent $0\nu\beta\beta$ -like mass terms $\langle m \rangle_{\alpha\beta}$ and CP-violating parts are associated with nine independent Jarlskog-like parameters $\mathcal{V}_{\alpha\beta}^{ij}$ (for $\alpha, \beta = e, \mu, \tau$ and $i, j = 1, 2, 3$). With the help of current neutrino oscillation data, we analyze the sensitivities of $|\langle m \rangle_{\alpha\beta}|$ and $\mathcal{V}_{\alpha\beta}^{ij}$ to the three CP-violating phases of U , and illustrate the salient features of six independent CP-violating asymmetries between $\nu_\alpha \rightarrow \bar{\nu}_\beta$ and $\bar{\nu}_\alpha \rightarrow \nu_\beta$ oscillations. As a by-product, the effects of the CP-violating phases on the LNV decays of doubly- and singly-charged Higgs bosons are reexamined by taking account of the unsuppressed value of θ_{13} . Such CP-conserving LNV processes can be complementary to the possible measurements of neutrino-antineutrino oscillations in the distant future.

PACS number(s): 14.60.Pq, 13.10.+q, 25.30.Pt

Keywords: Majorana phases, neutrino-antineutrino oscillations, CP violation

*E-mail: xingzz@ihep.ac.cn

†E-mail: zhouyeling@ihep.ac.cn

1 Introduction

Neutrinos are the most elusive fermions in the standard electroweak model, partly because they are electrically neutral and their masses are too small as compared with those charged leptons and quarks. The neutrality and smallness of neutrinos make it experimentally difficult to identify whether they are the Dirac or Majorana particles, but most theorists believe that massive neutrinos should have the Majorana nature (i.e., they are their own antiparticles [1]). To verify the Majorana nature of massive neutrinos, the most feasible way up to our current experimental techniques is to detect the neutrinoless double beta ($0\nu\beta\beta$) decay of some even-even nuclei [2]: $A(Z, N) \rightarrow A(Z + 2, N - 2) + 2e^-$, in which the lepton number is violated by two units. However, the $0\nu\beta\beta$ decay is a CP-conserving process and cannot directly be used to probe the Majorana CP-violating phases. Hence one has to consider other possible ways out of such a situation.

Given three massive neutrinos of the Majorana nature, the 3×3 Pontecorvo-Maki-Nakagawa-Sakata (PMNS) matrix U [3] can be parametrized in terms of three flavor mixing angles ($\theta_{12}, \theta_{13}, \theta_{23}$) and three CP-violating phases (δ, ρ, σ) as follows:

$$U = \begin{pmatrix} c_{12}c_{13} & s_{12}c_{13} & s_{13}e^{-i\delta} \\ -s_{12}c_{23} - c_{12}s_{13}s_{23}e^{i\delta} & c_{12}c_{23} - s_{12}s_{13}s_{23}e^{i\delta} & c_{13}s_{23} \\ s_{12}s_{23} - c_{12}s_{13}c_{23}e^{i\delta} & -c_{12}s_{23} - s_{12}s_{13}c_{23}e^{i\delta} & c_{13}c_{23} \end{pmatrix} \begin{pmatrix} e^{i\rho} & 0 & 0 \\ 0 & e^{i\sigma} & 0 \\ 0 & 0 & 1 \end{pmatrix}, \quad (1)$$

where $c_{ij} \equiv \cos\theta_{ij}$ and $s_{ij} \equiv \sin\theta_{ij}$ (for $ij = 12, 13, 23$). Although δ is usually referred to as the ‘‘Dirac’’ CP-violating phase which naturally appears in those lepton-number-conserving processes such as neutrino-neutrino and antineutrino-antineutrino oscillations, one should keep in mind that it is actually a Majorana phase like ρ or σ and can also show up in those lepton-number-violating (LNV) processes such as the $0\nu\beta\beta$ decay and neutrino-antineutrino oscillations. This point will soon become clear. So far all the three neutrino mixing angles have been measured to a good degree of accuracy in a number of solar, atmospheric, reactor and accelerator neutrino oscillation experiments [4]. A determination of the phase parameter δ via a measurement of the Jarlskog invariant $\mathcal{J} = c_{12}s_{12}c_{13}^2s_{13}c_{23}s_{23}\sin\delta$ [5] will be one of the major goals of the next-generation long-baseline neutrino oscillation experiments. The most challenging task is to detect the Majorana phases ρ and σ , which can only emerge in the LNV processes. As formulated by one of us in Ref. [6], it is *in principle* possible to determine all the three phases from the CP-violating asymmetries $\mathcal{A}_{\alpha\beta}$ between $\nu_\alpha \rightarrow \bar{\nu}_\beta$ and $\bar{\nu}_\alpha \rightarrow \nu_\beta$ oscillations. Nevertheless, a systematic study of this problem has been lacking.

The present work aims to go beyond Ref. [6] by carrying out a systematic analysis of the Majorana CP-violating phases in both neutrino-antineutrino oscillations and LNV decays of doubly- and singly-charged Higgs bosons based on the type-II seesaw mechanism [7]¹, in order to reveal their distinct properties which might be more or less associated with the observed matter-antimatter asymmetry of the Universe [9]. Our study is different from the previous ones at least in the following aspects:

- All the $0\nu\beta\beta$ -like mass terms $\langle m \rangle_{\alpha\beta}$ and the Jarlskog-like parameters $\mathcal{V}_{\alpha\beta}^{ij}$ (for $\alpha, \beta = e, \mu, \tau$ and $i, j = 1, 2, 3$), which measure the CP-conserving and CP-violating properties of Majorana neutrinos respectively, are analyzed in detail.
- The sensitivities of all the CP-violating asymmetries $\mathcal{A}_{\alpha\beta}$ to the phase parameters and the neutrino mass spectrum are discussed in a systematic way, and the ‘‘pseudo-Dirac’’ case with vanishing ρ and σ is also explored to illustrate why δ is of the Majorana nature.

¹As the $0\nu\beta\beta$ decay has been extensively discussed in the literature [8], here we shall not pay particular attention to it.

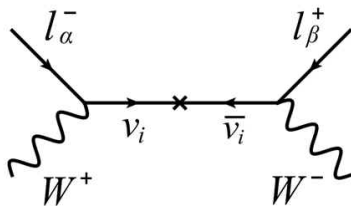


Figure 1: The Feynman diagram for $\nu_\alpha \rightarrow \bar{\nu}_\beta$ oscillations, where “ \times ” stands for the chirality flip in the neutrino propagator which is proportional to the mass m_i of the Majorana neutrino $\nu_i = \bar{\nu}_i$.

- The CP-conserving LNV decays of $H^{\pm\pm}$ and H^\pm bosons are reexamined by taking account of the unsuppressed value of θ_{13} reported by the Daya Bay [10] and RENO [11] Collaborations, and the dependence of their branching ratios on δ , ρ and σ is investigated.

Such a comprehensive analysis of the Majorana phases in CP-violating and CP-conserving LNV processes should be useful to illustrate how important they are in both lepton flavor mixing and CP violation and how difficult they are to be measured in reality.

The remaining parts of this paper are organized as follows. In section 2 we briefly review the salient features of three-flavor neutrino-antineutrino oscillations, including a concise discussion about the CP- and T-violating asymmetries. Section 3 is devoted to a detailed analysis of six independent $0\nu\beta\beta$ -like mass terms $\langle m \rangle_{\alpha\beta}$ and nine independent Jalskog-like parameters $\mathcal{V}_{\alpha\beta}^{ij}$ (for $\alpha, \beta = e, \mu, \tau$ and $i, j = 1, 2, 3$), which appear in the probabilities of $\nu_\alpha \rightarrow \bar{\nu}_\beta$ oscillations and their CP- or T-conjugate processes. A comparison between $\mathcal{V}_{\alpha\beta}^{ij}$ and \mathcal{J} is made by switching off the Majorana phases ρ and σ . As a by-product, the effects of three CP-violating phases on the LNV decays of doubly- and singly-charged Higgs bosons are also reexamined by taking account of the unsuppressed value of θ_{13} . In section 4 we carry out a systematic study of the sensitivities of six possible CP-violating asymmetries $\mathcal{A}_{\alpha\beta}$ to the three phase parameters, the absolute scale and hierarchies of three neutrino masses, and the ratio of the neutrino beam energy E to the baseline length L . Our numerical results illustrate the distinct roles of δ , ρ and σ or their combinations in neutrino-antineutrino oscillations. Section 5 is devoted to a summary of this work with some main conclusions.

2 Salient features of neutrino-antineutrino oscillations

Let us consider $\nu_\alpha \rightarrow \bar{\nu}_\beta$ oscillations (for $\alpha, \beta = e, \mu, \tau$), as schematically illustrated in Figure 1, where the production of ν_α and the detection of $\bar{\nu}_\beta$ are both governed by the standard weak charged-current interactions. The amplitudes of $\nu_\alpha \rightarrow \bar{\nu}_\beta$ transitions and their CP-conjugate processes $\bar{\nu}_\alpha \rightarrow \nu_\beta$ can be written as [6, 12]

$$\begin{aligned}
 A(\nu_\alpha \rightarrow \bar{\nu}_\beta) &= \sum_i \left[U_{\alpha i}^* U_{\beta i}^* \frac{m_i}{E} \exp\left(-i \frac{m_i^2}{2E} L\right) \right] K, \\
 A(\bar{\nu}_\alpha \rightarrow \nu_\beta) &= \sum_i \left[U_{\alpha i} U_{\beta i} \frac{m_i}{E} \exp\left(-i \frac{m_i^2}{2E} L\right) \right] \bar{K},
 \end{aligned} \tag{2}$$

where m_i denotes the mass of ν_i , E is the neutrino (or antineutrino) beam energy, L stands for the baseline length, K and \bar{K} are the kinematical factors independent of the index i (and satisfying $|K| = |\bar{K}|$). The helicity suppression in the transition between ν_i and $\bar{\nu}_i$ is characterized by m_i/E . The neutrino-antineutrino oscillation probabilities $P(\nu_\alpha \rightarrow \bar{\nu}_\beta) \equiv |A(\nu_\alpha \rightarrow \bar{\nu}_\beta)|^2$ and $P(\bar{\nu}_\alpha \rightarrow \nu_\beta) \equiv |A(\bar{\nu}_\alpha \rightarrow \nu_\beta)|^2$

turn out to be [6]

$$\begin{aligned}
P(\nu_\alpha \rightarrow \bar{\nu}_\beta) &= \frac{|K|^2}{E^2} \left[|\langle m \rangle_{\alpha\beta}|^2 - 4 \sum_{i<j} m_i m_j \mathcal{C}_{\alpha\beta}^{ij} \sin^2 \phi_{ji} + 2 \sum_{i<j} m_i m_j \mathcal{V}_{\alpha\beta}^{ij} \sin 2\phi_{ji} \right], \\
P(\bar{\nu}_\alpha \rightarrow \nu_\beta) &= \frac{|\bar{K}|^2}{E^2} \left[|\langle m \rangle_{\alpha\beta}|^2 - 4 \sum_{i<j} m_i m_j \mathcal{C}_{\alpha\beta}^{ij} \sin^2 \phi_{ji} - 2 \sum_{i<j} m_i m_j \mathcal{V}_{\alpha\beta}^{ij} \sin 2\phi_{ji} \right], \quad (3)
\end{aligned}$$

in which $\phi_{ji} \equiv \Delta m_{ji}^2 L / (4E)$ with $\Delta m_{ji}^2 \equiv m_j^2 - m_i^2$, the effective mass term $\langle m \rangle_{\alpha\beta}$ is defined as

$$\langle m \rangle_{\alpha\beta} \equiv \sum_i m_i U_{\alpha i} U_{\beta i}, \quad (4)$$

and the CP-conserving and CP-violating contributions of the PMNS flavor mixing matrix elements are described by

$$\begin{aligned}
\mathcal{C}_{\alpha\beta}^{ij} &\equiv \text{Re} (U_{\alpha i} U_{\beta i} U_{\alpha j}^* U_{\beta j}^*), \\
\mathcal{V}_{\alpha\beta}^{ij} &\equiv \text{Im} (U_{\alpha i} U_{\beta i} U_{\alpha j}^* U_{\beta j}^*), \quad (5)
\end{aligned}$$

with the Greek and Latin subscripts running over (e, μ, τ) and $(1, 2, 3)$, respectively. Note that $\langle m \rangle_{\alpha\beta}$ is the (α, β) element of the Majorana neutrino mass matrix $M_\nu = U \widehat{M}_\nu U^T$ with $\widehat{M}_\nu \equiv \text{Diag}\{m_1, m_2, m_3\}$ in the flavor basis where the charged-lepton mass matrix is diagonal, and thus $\langle m \rangle_{\alpha\beta} = \langle m \rangle_{\beta\alpha}$ holds as a result of the symmetry of M_ν . Because $\langle m \rangle_{ee}$ is simply the effective mass term of the $0\nu\beta\beta$ decay, we refer to $\langle m \rangle_{\alpha\beta}$ as the $0\nu\beta\beta$ -like mass terms. Similarly, the CP- and T-violating quantities $\mathcal{V}_{\alpha\beta}^{ij}$ are referred to as the Jarlskog-like parameters.

By definition, the CP-conserving quantities $\mathcal{C}_{\alpha\beta}^{ij}$ satisfy $\mathcal{C}_{\alpha\beta}^{ij} = \mathcal{C}_{\beta\alpha}^{ij} = \mathcal{C}_{\alpha\beta}^{ji} = \mathcal{C}_{\beta\alpha}^{ji}$. In addition, $\mathcal{C}_{\alpha\beta}^{ij}$ and $\langle m \rangle_{\alpha\beta}$ are related to each other through

$$|\langle m \rangle_{\alpha\beta}|^2 = \sum_i m_i^2 \mathcal{C}_{\alpha\beta}^{ii} + 2 \sum_{i<j} m_i m_j \mathcal{C}_{\alpha\beta}^{ij}. \quad (6)$$

This relation allows us to rewrite Eq. (3) as

$$\begin{aligned}
P(\nu_\alpha \rightarrow \bar{\nu}_\beta) &= \frac{|K|^2}{E^2} \left[\sum_i m_i^2 \mathcal{C}_{\alpha\beta}^{ii} + 2 \sum_{i<j} m_i m_j \left(\mathcal{C}_{\alpha\beta}^{ij} \cos 2\phi_{ji} + \mathcal{V}_{\alpha\beta}^{ij} \sin 2\phi_{ji} \right) \right], \\
P(\bar{\nu}_\alpha \rightarrow \nu_\beta) &= \frac{|\bar{K}|^2}{E^2} \left[\sum_i m_i^2 \mathcal{C}_{\alpha\beta}^{ii} + 2 \sum_{i<j} m_i m_j \left(\mathcal{C}_{\alpha\beta}^{ij} \cos 2\phi_{ji} - \mathcal{V}_{\alpha\beta}^{ij} \sin 2\phi_{ji} \right) \right]. \quad (7)
\end{aligned}$$

The unitarity of the PMNS matrix U leads us to the relations

$$\begin{aligned}
\sum_\alpha \mathcal{C}_{\alpha\beta}^{ij} &= \sum_\beta \mathcal{C}_{\alpha\beta}^{ij} = 0, \\
\sum_\alpha \mathcal{V}_{\alpha\beta}^{ij} &= \sum_\beta \mathcal{V}_{\alpha\beta}^{ij} = 0, \quad (8)
\end{aligned}$$

for $i \neq j$. Then we arrive at the following sum rule for the probabilities of $\nu_\alpha \rightarrow \bar{\nu}_\beta$ and $\bar{\nu}_\alpha \rightarrow \nu_\beta$ oscillations:

$$\sum_\beta P(\nu_\alpha \rightarrow \bar{\nu}_\beta) = \sum_\beta P(\bar{\nu}_\alpha \rightarrow \nu_\beta) = \frac{|K|^2}{E^2} |\langle m \rangle_\alpha|^2, \quad (9)$$

where

$$|\langle m \rangle_\alpha|^2 \equiv \sum_i m_i^2 |U_{\alpha i}|^2, \quad (10)$$

which is actually the (α, α) element of $M_\nu M_\nu^\dagger$. In particular, $\langle m \rangle_e$ is just the effective mass term appearing in the rate of the tritium beta decay ${}^3_1\text{H} \rightarrow {}^3_2\text{He} + e^- + \bar{\nu}_e$. In comparison with Eq. (9), the so-called *zero-distance effect* of neutrino-antineutrino oscillations at $L = 0$ is given by

$$P(\nu_\alpha \rightarrow \bar{\nu}_\beta) = P(\bar{\nu}_\alpha \rightarrow \nu_\beta) = \frac{|K|^2}{E^2} |\langle m \rangle_{\alpha\beta}|^2. \quad (11)$$

Because of $m_i \ll E$, the effects in both Eqs. (9) and (11) are extremely suppressed.

Thanks to CPT invariance, it is easy to check that $P(\nu_\alpha \rightarrow \bar{\nu}_\beta) = P(\nu_\beta \rightarrow \bar{\nu}_\alpha)$ and $P(\bar{\nu}_\alpha \rightarrow \nu_\beta) = P(\bar{\nu}_\beta \rightarrow \nu_\alpha)$ hold. Hence the T-violating asymmetry between $\nu_\alpha \rightarrow \bar{\nu}_\beta$ and $\bar{\nu}_\beta \rightarrow \nu_\alpha$ oscillations must be exactly equal to the CP-violating asymmetry between $\nu_\alpha \rightarrow \bar{\nu}_\beta$ and $\bar{\nu}_\alpha \rightarrow \nu_\beta$ oscillations. To eliminate the $|K|^2/E^2$ and $|\bar{K}|^2/E^2$ factors, we define the CP-violating asymmetry between $\nu_\alpha \rightarrow \bar{\nu}_\beta$ and $\bar{\nu}_\alpha \rightarrow \nu_\beta$ oscillations as the ratio of the difference $P(\nu_\alpha \rightarrow \bar{\nu}_\beta) - P(\bar{\nu}_\alpha \rightarrow \nu_\beta)$ to the sum $P(\nu_\alpha \rightarrow \bar{\nu}_\beta) + P(\bar{\nu}_\alpha \rightarrow \nu_\beta)$, denoted by $\mathcal{A}_{\alpha\beta}$ [6]. Therefore,

$$\begin{aligned} \mathcal{A}_{\alpha\beta} &= \frac{2 \sum_{i<j} m_i m_j \mathcal{V}_{\alpha\beta}^{ij} \sin 2\phi_{ji}}{\sum_i m_i^2 \mathcal{C}_{\alpha\beta}^{ii} + 2 \sum_{i<j} m_i m_j \mathcal{C}_{\alpha\beta}^{ij} \cos 2\phi_{ji}} \\ &= \frac{2 \sum_{i<j} m_i m_j \mathcal{V}_{\alpha\beta}^{ij} \sin 2\phi_{ji}}{|\langle m \rangle_{\alpha\beta}|^2 - 4 \sum_{i<j} m_i m_j \mathcal{C}_{\alpha\beta}^{ij} \sin^2 \phi_{ji}}. \end{aligned} \quad (12)$$

We see that $\mathcal{A}_{\alpha\beta} = \mathcal{A}_{\beta\alpha}$ holds, so only six of the nine CP-violating asymmetries are independent and nontrivial. As pointed out in Ref. [6], Eq. (12) will not be much simplified even if $\alpha = \beta$ is taken. Namely, the $\nu_\alpha \rightarrow \bar{\nu}_\alpha$ oscillation is actually a kind of ‘‘appearance’’ process and thus it can accommodate the CP- and T-violating effects.

It is absolutely true that a measurement of neutrino-antineutrino oscillations is far beyond the capability of nowadays experimental technology. The main problem arises from the helicity suppression proportional to m_i/E . Given the fact that the neutrino masses are constrained to be below the eV scale but those currently available neutrino sources all have $E \gtrsim \mathcal{O}(1)$ MeV, the neutrino-antineutrino oscillation probabilities are formidably suppressed by the factor $m_i^2/E^2 \lesssim \mathcal{O}(10^{-12})$. A naive suggestion is to lower E and hence enhance m_i/E in a thought experiment [6], implying that the baseline length of such an experiment must be very short. This point can be more clearly seen from an estimate of the typical oscillation lengths by taking $E \sim \mathcal{O}(10)$ keV for example ²:

$$\begin{aligned} (1) \quad L_{31}^{\text{osc}} &\simeq L_{32}^{\text{osc}} \simeq \frac{E}{10 \text{ keV}} \times 10 \text{ m}, \\ (2) \quad L_{21}^{\text{osc}} &\simeq \frac{E}{10 \text{ keV}} \times 330 \text{ m}, \end{aligned} \quad (13)$$

²For example, the Mössbauer electron antineutrinos are the $E = 18.6$ keV $\bar{\nu}_e$ events which could be used to do an oscillation experiment [13]. In this case we have $L_{31}^{\text{osc}} \simeq 18$ m and $L_{21}^{\text{osc}} \simeq 600$ m, and the size of the detector could be as small as $\mathcal{O}(10^{-2})$ m by using metal crystals.

corresponding to $\Delta m_{21}^2 \simeq 7.5 \times 10^{-5} \text{ eV}^2$ and $|\Delta m_{31}^2| \simeq |\Delta m_{32}^2| \simeq 2.4 \times 10^{-3} \text{ eV}^2$, respectively. In this case, however, the sizes of the neutrino (or antineutrino) source and the detector must be much smaller than the ones characterized by L_{21}^{osc} and (or) $L_{31}^{\text{osc}} \simeq L_{32}^{\text{osc}}$. Note that the result in Eq. (11) is essentially equivalent to the $L_{ji}^{\text{osc}} \gg L$ case. If $L_{ji}^{\text{osc}} \ll L$, instead, the Δm_{ji}^2 -dependent oscillation terms will be averaged out and then the probabilities will be simplified to

$$P(\nu_\alpha \rightarrow \bar{\nu}_\beta) = P(\bar{\nu}_\alpha \rightarrow \nu_\beta) = \frac{|K|^2}{E^2} \sum_i m_i^2 \mathcal{C}_{\alpha\beta}^{ii}. \quad (14)$$

This CP-conserving result can be compared with the ones in Eqs. (9) and (11).

3 Properties and profiles of $\mathcal{V}_{\alpha\beta}^{ij}$ and $\langle m \rangle_{\alpha\beta}$

As shown in section 2, neutrino-antineutrino oscillations are closely associated with the effective mass terms $\langle m \rangle_{\alpha\beta}$ and the CP-violating quantities $\mathcal{V}_{\alpha\beta}^{ij}$. The former may also appear in some other LNV processes in which CP and T symmetries are conserved. Let us explore the analytical properties and numerical profiles of $\mathcal{V}_{\alpha\beta}^{ij}$ and $\langle m \rangle_{\alpha\beta}$ in some detail in this section.

3.1 The Jarlskog-like parameters $\mathcal{V}_{\alpha\beta}^{ij}$

It is well known that the strength of CP and T violation in normal neutrino-neutrino and antineutrino-antineutrino oscillations is measured by a single rephasing-invariant quantity, the so-called Jarlskog parameter \mathcal{J} [5], defined through

$$\text{Im}(U_{\alpha i} U_{\beta j} U_{\alpha j}^* U_{\beta i}^*) = \mathcal{J} \sum_\gamma \epsilon_{\alpha\beta\gamma} \sum_k \epsilon_{ijk}, \quad (15)$$

where U is the PMNS matrix. In terms of the standard parametrization of U given in Eq. (1), we have

$$\mathcal{J} = c_{12} s_{12} c_{13}^2 s_{13} c_{23} s_{23} \sin \delta. \quad (16)$$

Therefore, a measurement of the CP-violating asymmetry between $P(\nu_\alpha \rightarrow \nu_\beta)$ and $P(\bar{\nu}_\alpha \rightarrow \bar{\nu}_\beta)$ or the T-violating asymmetry between $P(\nu_\alpha \rightarrow \nu_\beta)$ and $P(\nu_\beta \rightarrow \nu_\alpha)$ can only probe the ‘‘Dirac’’ phase δ [14]. In contrast, the other two phases of U (i.e., ρ and σ) may contribute to the Jarlskog-like quantities $\mathcal{V}_{\alpha\beta}^{ij}$ defined in Eq. (5), and thus they can in principle be measured in neutrino-antineutrino oscillations.

By definition, the Jarlskog-like parameters $\mathcal{V}_{\alpha\beta}^{ij}$ satisfy the relations

$$\mathcal{V}_{\alpha\beta}^{ij} = \mathcal{V}_{\beta\alpha}^{ij} = -\mathcal{V}_{\alpha\beta}^{ji} = -\mathcal{V}_{\beta\alpha}^{ji}, \quad (17)$$

and $\mathcal{V}_{\alpha\beta}^{ii} = 0$; but $\mathcal{V}_{\alpha\alpha}^{ij} \neq 0$ for $i \neq j$. With the help of Eq. (17), one may express $\mathcal{V}_{\alpha\beta}^{ij}$ in terms of three different $\mathcal{V}_{\alpha\alpha}^{ij}$ as follows:

$$\begin{aligned} \mathcal{V}_{e\mu}^{ij} &= \frac{1}{2} (\mathcal{V}_{\tau\tau}^{ij} - \mathcal{V}_{ee}^{ij} - \mathcal{V}_{\mu\mu}^{ij}), \\ \mathcal{V}_{e\tau}^{ij} &= \frac{1}{2} (\mathcal{V}_{\mu\mu}^{ij} - \mathcal{V}_{ee}^{ij} - \mathcal{V}_{\tau\tau}^{ij}), \\ \mathcal{V}_{\mu\tau}^{ij} &= \frac{1}{2} (\mathcal{V}_{ee}^{ij} - \mathcal{V}_{\mu\mu}^{ij} - \mathcal{V}_{\tau\tau}^{ij}). \end{aligned} \quad (18)$$

This result implies that only nine $\mathcal{V}_{\alpha\beta}^{ij}$ are independent.

To see the explicit dependence of each $\mathcal{V}_{\alpha\beta}^{ij}$ on the CP-violating phases, let us calculate $\mathcal{V}_{\alpha\alpha}^{ij}$ in the standard parametrization of U given by Eq. (1). We obtain

$$\begin{aligned}\mathcal{V}_{ee}^{12} &= c_{12}^2 s_{12}^2 c_{13}^4 \sin 2(\rho - \sigma) , \\ \mathcal{V}_{ee}^{13} &= c_{12}^2 c_{13}^2 s_{13}^2 \sin 2(\delta + \rho) , \\ \mathcal{V}_{ee}^{23} &= s_{12}^2 c_{13}^2 s_{13}^2 \sin 2(\delta + \sigma) ;\end{aligned}\tag{19}$$

and

$$\begin{aligned}\mathcal{V}_{\mu\mu}^{12} &= c_{12}^2 s_{12}^2 (c_{23}^4 - 4s_{13}^2 c_{23}^2 s_{23}^2 + s_{13}^4 s_{23}^4) \sin 2(\rho - \sigma) \\ &\quad + 2c_{12} s_{12} s_{13} c_{23} s_{23} (c_{23}^2 - s_{13}^2 s_{23}^2) [c_{12}^2 \sin(2\rho - 2\sigma + \delta) - s_{12}^2 \sin(2\rho - 2\sigma - \delta)] \\ &\quad + s_{13}^2 c_{23}^2 s_{23}^2 [c_{12}^4 \sin 2(\rho - \sigma + \delta) + s_{12}^4 \sin 2(\rho - \sigma - \delta)] , \\ \mathcal{V}_{\mu\mu}^{13} &= c_{13}^2 s_{23}^2 [s_{12}^2 c_{23}^2 \sin 2\rho + 2c_{12} s_{12} s_{13} c_{23} s_{23} \sin(\delta + 2\rho) + c_{12}^2 s_{13}^2 s_{23}^2 \sin 2(\delta + \rho)] , \\ \mathcal{V}_{\mu\mu}^{23} &= c_{13}^2 s_{23}^2 [c_{12}^2 c_{23}^2 \sin 2\sigma - 2c_{12} s_{12} s_{13} c_{23} s_{23} \sin(\delta + 2\sigma) + s_{12}^2 s_{13}^2 s_{23}^2 \sin 2(\delta + \sigma)] ;\end{aligned}\tag{20}$$

and

$$\begin{aligned}\mathcal{V}_{\tau\tau}^{12} &= c_{12}^2 s_{12}^2 (s_{23}^4 - 4s_{13}^2 c_{23}^2 s_{23}^2 + s_{13}^4 c_{23}^4) \sin 2(\rho - \sigma) \\ &\quad - 2c_{12} s_{12} s_{13} c_{23} s_{23} (s_{23}^2 - s_{13}^2 c_{23}^2) [c_{12}^2 \sin(2\rho - 2\sigma + \delta) - s_{12}^2 \sin(2\rho - 2\sigma - \delta)] \\ &\quad + s_{13}^2 c_{23}^2 s_{23}^2 [c_{12}^4 \sin 2(\rho - \sigma + \delta) + s_{12}^4 \sin 2(\rho - \sigma - \delta)] , \\ \mathcal{V}_{\tau\tau}^{13} &= c_{13}^2 c_{23}^2 [s_{12}^2 s_{23}^2 \sin 2\rho - 2c_{12} s_{12} s_{13} c_{23} s_{23} \sin(\delta + 2\rho) + c_{12}^2 s_{13}^2 c_{23}^2 \sin 2(\delta + \rho)] , \\ \mathcal{V}_{\tau\tau}^{23} &= c_{13}^2 c_{23}^2 [c_{12}^2 s_{23}^2 \sin 2\sigma + 2c_{12} s_{12} s_{13} c_{23} s_{23} \sin(\delta + 2\sigma) + s_{12}^2 s_{13}^2 c_{23}^2 \sin 2(\delta + \sigma)] .\end{aligned}\tag{21}$$

Taking account of Eq. (18), we can immediately write out the explicit expressions of $\mathcal{V}_{\alpha\beta}^{ij}$ (for $\alpha \neq \beta$) with the help of Eqs. (19)–(21):

$$\begin{aligned}\mathcal{V}_{e\mu}^{12} &= -c_{12}^2 s_{12}^2 c_{13}^2 (c_{23}^2 - s_{13}^2 s_{23}^2) \sin 2(\rho - \sigma) \\ &\quad - c_{12} s_{12} c_{13}^2 s_{13} c_{23} s_{23} [c_{12}^2 \sin(2\rho - 2\sigma + \delta) - s_{12}^2 \sin(2\rho - 2\sigma - \delta)] , \\ \mathcal{V}_{e\mu}^{13} &= -c_{12} c_{13}^2 s_{13} s_{23} [s_{12} c_{23} \sin(\delta + 2\rho) - c_{12} s_{13} s_{23} \sin 2(\delta + \rho)] , \\ \mathcal{V}_{e\mu}^{23} &= +s_{12} c_{13}^2 s_{13} s_{23} [c_{12} c_{23} \sin(\delta + 2\sigma) - s_{12} s_{13} s_{23} \sin 2(\delta + \sigma)] ;\end{aligned}\tag{22}$$

and

$$\begin{aligned}\mathcal{V}_{e\tau}^{12} &= c_{12}^2 s_{12}^2 c_{13}^2 (c_{23}^2 s_{13}^2 - s_{23}^2) \sin 2(\rho - \sigma) \\ &\quad + c_{12} s_{12} c_{13}^2 s_{13} c_{23} s_{23} [c_{12}^2 \sin(2\rho - 2\sigma + \delta) - s_{12}^2 \sin(2\rho - 2\sigma - \delta)] , \\ \mathcal{V}_{e\tau}^{13} &= +c_{12} c_{13}^2 s_{13} c_{23} [s_{12} s_{23} \sin(\delta + 2\rho) - c_{12} s_{13} c_{23} \sin 2(\delta + \rho)] , \\ \mathcal{V}_{e\tau}^{23} &= -s_{12} c_{13}^2 s_{13} c_{23} [c_{12} s_{23} \sin(\delta + 2\sigma) + s_{12} s_{13} c_{23} \sin 2(\delta + \sigma)] ;\end{aligned}\tag{23}$$

and

$$\begin{aligned}\mathcal{V}_{\mu\tau}^{12} &= -c_{12}^2 s_{12}^2 [c_{23}^4 s_{13}^2 - (1 + s_{13}^2)^2 c_{23}^2 s_{23}^2 + s_{13}^2 s_{23}^4] \sin 2(\rho - \sigma) \\ &\quad - c_{12} s_{12} s_{13} c_{23} s_{23} (1 + s_{13}^2) (c_{23}^2 - s_{23}^2) [c_{12}^2 \sin(2\rho - 2\sigma + \delta) - s_{12}^2 \sin(2\rho - 2\sigma - \delta)] \\ &\quad - s_{13}^2 c_{23}^2 s_{23}^2 [c_{12}^4 \sin 2(\rho - \sigma + \delta) + s_{12}^4 \sin 2(\rho - \sigma - \delta)] , \\ \mathcal{V}_{\mu\tau}^{13} &= c_{13}^2 c_{23} s_{23} [-s_{12}^2 c_{23} s_{23} \sin 2\rho + c_{12} s_{12} s_{13} (c_{23}^2 - s_{23}^2) \sin(\delta + 2\rho) + c_{12}^2 s_{13}^2 c_{23} s_{23} \sin 2(\delta + \rho)] , \\ \mathcal{V}_{\mu\tau}^{23} &= c_{13}^2 c_{23} s_{23} [-c_{12}^2 c_{23} s_{23} \sin 2\sigma - c_{12} s_{12} s_{13} (c_{23}^2 - s_{23}^2) \sin(\delta + 2\sigma) + s_{12}^2 s_{13}^2 c_{23} s_{23} \sin 2(\delta + \sigma)] .\end{aligned}\tag{24}$$

Table 1: The simplified expressions of the Jarlskog-like parameters $\mathcal{V}_{\alpha\beta}^{ij}$ and their relations with the Jarlskog parameter \mathcal{J} in the $\rho = \sigma = 0$ limit. Their typical numerical results are obtained by inputting $\theta_{12} \simeq 33.4^\circ$, $\theta_{13} \simeq 8.66^\circ$ and $\theta_{23} \simeq 40.0^\circ$ [15] in the $\delta = 45^\circ$ and $\delta = 90^\circ$ cases.

Jarlskog-like parameter	$\delta = 45^\circ$	$\delta = 90^\circ$
$\mathcal{V}_{ee}^{12} = 0$	0	0
$\mathcal{V}_{ee}^{13} = c_{12}^2 c_{13}^2 s_{13}^2 \sin 2\delta$	+0.016	0
$\mathcal{V}_{ee}^{23} = s_{12}^2 c_{13}^2 s_{13}^2 \sin 2\delta$	+0.0067	0
$\mathcal{V}_{\mu\mu}^{12} = [2\mathcal{J}(c_{23}^2 - s_{13}^2 s_{23}^2) + (\mathcal{V}_{ee}^{13} - \mathcal{V}_{ee}^{23})c_{23}^2 s_{23}^2] / c_{13}^2$	+0.030	+0.039
$\mathcal{V}_{\mu\mu}^{13} = 2\mathcal{J}s_{23}^2 + \mathcal{V}_{ee}^{13}s_{23}^4$	+0.022	+0.028
$\mathcal{V}_{\mu\mu}^{23} = -2\mathcal{J}s_{23}^2 + \mathcal{V}_{ee}^{23}s_{23}^4$	-0.018	-0.028
$\mathcal{V}_{\tau\tau}^{12} = [2\mathcal{J}(s_{13}^2 c_{23}^2 - s_{23}^2) + (\mathcal{V}_{ee}^{13} - \mathcal{V}_{ee}^{23})c_{23}^2 s_{23}^2] / c_{13}^2$	-0.017	-0.027
$\mathcal{V}_{\tau\tau}^{13} = -2\mathcal{J}c_{23}^2 + \mathcal{V}_{ee}^{13}c_{23}^4$	-0.022	-0.039
$\mathcal{V}_{\tau\tau}^{23} = 2\mathcal{J}c_{23}^2 + \mathcal{V}_{ee}^{23}c_{23}^4$	+0.030	+0.039
$\mathcal{V}_{e\mu}^{12} = -\mathcal{J}$	-0.024	-0.033
$\mathcal{V}_{e\mu}^{13} = -\mathcal{J} + \mathcal{V}_{ee}^{13}s_{23}^2$	-0.030	-0.033
$\mathcal{V}_{e\mu}^{23} = \mathcal{J} - \mathcal{V}_{ee}^{13}s_{23}^2$	+0.021	+0.033
$\mathcal{V}_{e\tau}^{12} = \mathcal{J}$	+0.024	+0.033
$\mathcal{V}_{e\tau}^{13} = \mathcal{J} - \mathcal{V}_{ee}^{13}c_{23}^2$	+0.014	+0.033
$\mathcal{V}_{e\tau}^{23} = -\mathcal{J} - \mathcal{V}_{ee}^{23}c_{23}^2$	-0.028	-0.033
$\mathcal{V}_{\mu\tau}^{12} = [\mathcal{J}(1 + s_{13}^2)(s_{23}^2 - c_{23}^2) - (\mathcal{V}_{ee}^{13} - \mathcal{V}_{ee}^{23})c_{23}^2 s_{23}^2] / c_{13}^2$	-0.0064	-0.0060
$\mathcal{V}_{\mu\tau}^{13} = \mathcal{J}(c_{23}^2 - s_{23}^2) + \mathcal{V}_{ee}^{13}c_{23}^2 s_{23}^2$	+0.0078	+0.0058
$\mathcal{V}_{\mu\tau}^{23} = \mathcal{J}(s_{23}^2 - c_{23}^2) + \mathcal{V}_{ee}^{23}c_{23}^2 s_{23}^2$	-0.0025	-0.0058

Similar expressions for $\mathcal{C}_{\alpha\beta}^{ij}$ have been listed in Appendix A. These results clearly tell us how the CP-violating quantities $\mathcal{V}_{\alpha\beta}^{ij}$ depend on the CP-violating phases δ , ρ and σ : (a) each $\mathcal{V}_{\alpha\beta}^{12}$ is a function of $\rho - \sigma$ and δ (the only exception is \mathcal{V}_{ee}^{12} , which only involves $\rho - \sigma$); (b) each $\mathcal{V}_{\alpha\beta}^{13}$ is a function of ρ and δ ; and (c) each $\mathcal{V}_{\alpha\beta}^{23}$ is a function of σ and δ . The following extreme cases are particularly interesting.

- In the $\delta = 0$ (or π) limit, $\mathcal{J} = 0$ holds, but all the $\mathcal{V}_{\alpha\beta}^{ij}$ are in general nonvanishing. In this special case there will be no CP or T violation in normal neutrino-neutrino and antineutrino-antineutrino oscillations, but large CP or T violation in neutrino-antineutrino oscillations is possible.
- In the $\theta_{13} = 0$ limit, $\mathcal{J} = 0$ holds, so does

$$\mathcal{V}_{ee}^{13} = \mathcal{V}_{ee}^{23} = \mathcal{V}_{e\mu}^{13} = \mathcal{V}_{e\mu}^{23} = \mathcal{V}_{e\tau}^{13} = \mathcal{V}_{e\tau}^{23} = 0, \quad (25)$$

simply because all of them involve the $U_{e3} = s_{13}e^{-i\delta}$ element. Those nonvanishing Jarlskog-like parameters depend on either ρ or σ , or their difference $\rho - \sigma$. However, such an extreme case is not favored by the recent reactor antineutrino oscillation data (i.e., $\theta_{13} \simeq 9^\circ$ [10, 11]).

- In the $\rho = \sigma = 0$ limit, which looks like a “pseudo-Dirac” case with a single CP-violating parameter δ , we obtain $\mathcal{V}_{ee}^{12} = 0$, $\mathcal{V}_{ee}^{13} = c_{12}^2 c_{13}^2 s_{13}^2 \sin 2\delta$ and $\mathcal{V}_{ee}^{23} = s_{12}^2 c_{13}^2 s_{13}^2 \sin 2\delta$. The other fifteen $\mathcal{V}_{\alpha\beta}^{ij}$ can all be given in terms of \mathcal{J} , \mathcal{V}_{ee}^{13} and \mathcal{V}_{ee}^{23} , as listed in Table 1. We see $\mathcal{V}_{e\tau}^{12} = -\mathcal{V}_{e\mu}^{12} = \mathcal{J}$,

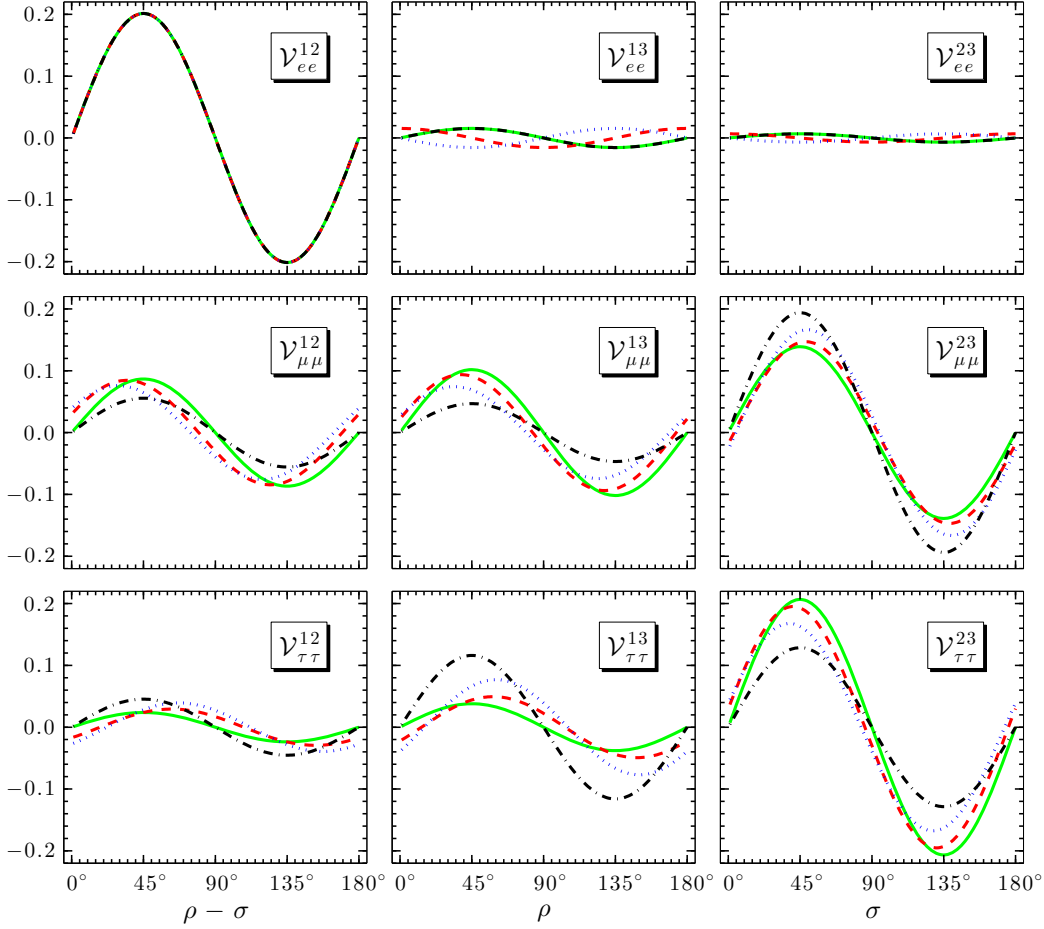


Figure 2: The Jarlskog-like parameters $\mathcal{V}_{\alpha\alpha}^{ij}$ changing with the CP-violating phases. The green solid, red dashed, blue dotted and black dashed-dotted lines correspond to $\delta = 0^\circ, 45^\circ, 90^\circ$ and 180° , respectively. The typical inputs are $\theta_{12} \simeq 33.4^\circ$, $\theta_{13} \simeq 8.66^\circ$ and $\theta_{23} \simeq 40.0^\circ$ [15].

and the other nonvanishing $\mathcal{V}_{\alpha\beta}^{ij}$ may also receive the higher-order contributions proportional to $s_{13}^2 \sin 2\delta$ (i.e., the \mathcal{V}_{ee}^{13} and \mathcal{V}_{ee}^{23} terms). In this case the Jarlskog parameter \mathcal{J} governs CP and T violation in both normal neutrino-neutrino (or antineutrino-antineutrino) oscillations and neutrino-antineutrino oscillations.

Of course, it is possible to relate $\mathcal{V}_{\alpha\beta}^{ij}$ to \mathcal{J} in some other special cases. For example, $\rho = \sigma = -\delta$ leads to $\mathcal{V}_{e\tau}^{12} = -\mathcal{V}_{e\tau}^{13} = \mathcal{V}_{e\tau}^{23} = -\mathcal{V}_{e\mu}^{12} = \mathcal{V}_{e\mu}^{13} = -\mathcal{V}_{e\mu}^{23} = \mathcal{J}$.

We proceed to illustrate the numerical dependence of $\mathcal{V}_{\alpha\beta}^{ij}$ on ρ , σ and δ by taking $\theta_{12} \simeq 33.4^\circ$, $\theta_{13} \simeq 8.66^\circ$ and $\theta_{23} \simeq 40.0^\circ$ as the typical inputs [15]. As the ‘‘Dirac’’ phase δ is expected to be determined earlier than the Majorana phases ρ and σ , one may fix the value of δ (for example, $\delta = 0^\circ, 45^\circ, 90^\circ$ or 180°) to show how $\mathcal{V}_{\alpha\beta}^{ij}$ can change with $\rho - \sigma$, ρ or σ . Our numerical results of $\mathcal{V}_{\alpha\beta}^{ij}$ for the $\alpha = \beta$ and $\alpha \neq \beta$ cases are shown in Figures 2 and 3, respectively. In addition, the magnitude of each $\mathcal{V}_{\alpha\beta}^{ij}$ in the $\rho = \sigma = 0$ limit is illustrated in Table 1. Some comments are in order.

- It is amazing that \mathcal{V}_{ee}^{12} , $\mathcal{V}_{\mu\mu}^{23}$, $\mathcal{V}_{\tau\tau}^{23}$ and $\mathcal{V}_{\mu\tau}^{23}$ can maximally reach about 20% in magnitude. In comparison, $\mathcal{J} \leq 1/(6\sqrt{3}) \simeq 9.6\%$ constrains the strength of CP and T violation in normal neutrino-neutrino oscillations [16]. The reason for possible largeness of the above four Jarlskog-like parameters is simply that their leading terms are only slightly suppressed by s_{12}^2 or s_{23}^2 .

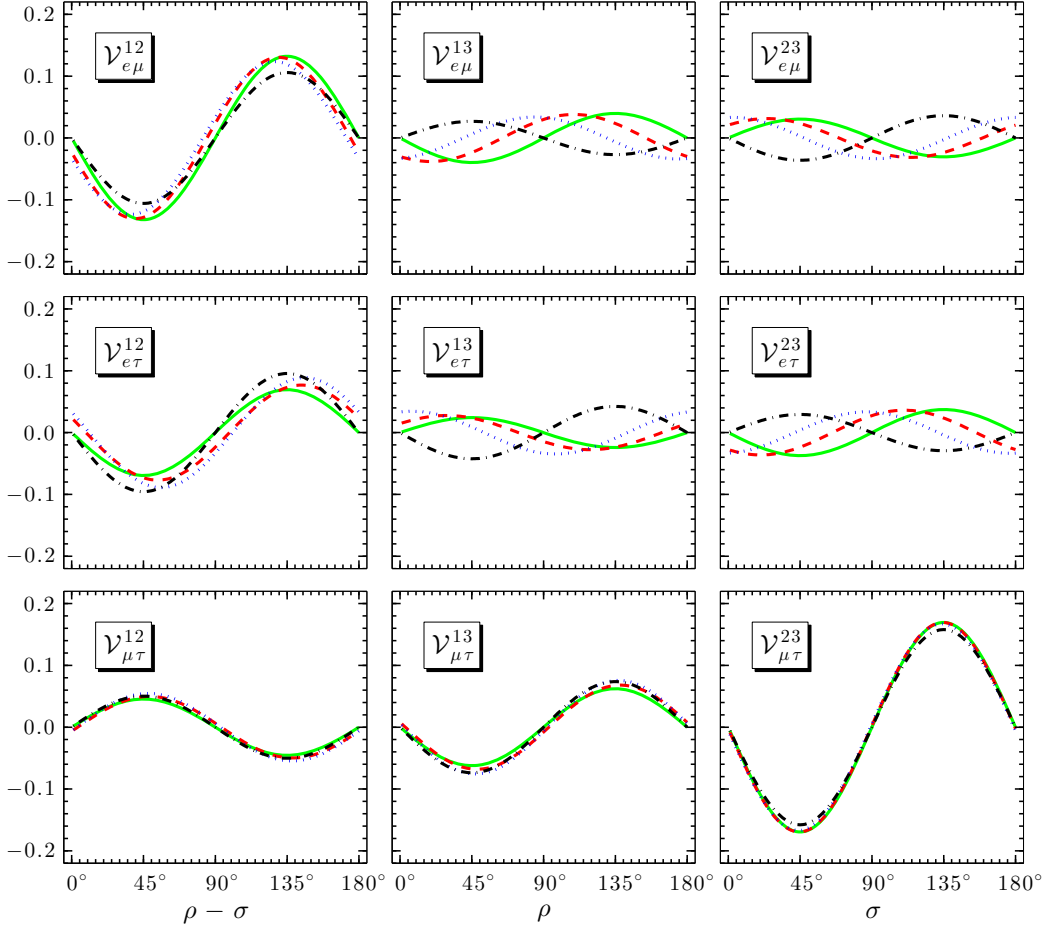


Figure 3: The Jarlskog-like parameters $\mathcal{V}_{\alpha\beta}^{ij}$ (for $\alpha \neq \beta$) changing with the CP-violating phases. The green solid, red dashed, blue dotted and black dashed-dotted lines correspond to $\delta = 0^\circ, 45^\circ, 90^\circ$ and 180° , respectively. The typical inputs are $\theta_{12} \simeq 33.4^\circ, \theta_{13} \simeq 8.66^\circ$ and $\theta_{23} \simeq 40.0^\circ$ [15].

- The magnitudes of \mathcal{V}_{ee}^{13} and \mathcal{V}_{ee}^{23} are strongly suppressed, because both of them are proportional to $s_{13}^2 \simeq 2.3\%$. We see that the magnitudes of $\mathcal{V}_{e\mu}^{13}$, $\mathcal{V}_{e\mu}^{23}$, $\mathcal{V}_{e\tau}^{13}$ and $\mathcal{V}_{e\tau}^{23}$ are modest, since their leading terms are comparable with \mathcal{J} . In other words, they are essentially constrained to be $\lesssim 10\%$.
- \mathcal{V}_{ee}^{12} has nothing to do with the “Dirac” phase δ , as one can see in Eq. (19). The dependence of $\mathcal{V}_{\mu\tau}^{12}$, $\mathcal{V}_{\mu\tau}^{13}$ and $\mathcal{V}_{\mu\tau}^{23}$ on δ is very weak, because this dependence is suppressed either by the factor $s_{13}^2 (c_{23}^2 - s_{23}^2) \simeq 2.6\%$ or by the factor $s_{13}^2 \simeq 2.3\%$ as shown in Eq. (24).
- The “pseudo-Dirac” case illustrated in Table 1 is interesting in the sense that appreciable CP- and T-violating effects are expected to show up in neutrino-antineutrino oscillations even the Majorana phases ρ and σ vanish. Namely, the Majorana neutrinos with only the “Dirac” CP-violating phase behave very differently from the Dirac neutrinos ³.

Therefore, it is in principle possible to determine all the three CP-violating phases in neutrino-antineutrino oscillations, in which the strength of CP and T violation is governed by $\mathcal{V}_{\alpha\beta}^{ij}$, whose maximal magnitudes could be larger than that of \mathcal{J} by a factor of two or so. We shall come back to this point in section 4 to analyze the CP-violating asymmetries between $\nu_\alpha \rightarrow \bar{\nu}_\beta$ and $\bar{\nu}_\alpha \rightarrow \nu_\beta$ oscillations.

³This point can also be seen by examining their distinct renormalization-group running effects [17].

3.2 The effective mass terms $\langle m \rangle_{\alpha\beta}$

The effective mass terms $\langle m \rangle_{\alpha\beta}$ defined in Eq. (4) are important to understand the origin of neutrino masses, since they are simply the (α, β) elements of the symmetric Majorana neutrino mass matrix M_ν in the basis where the flavor eigenstates of three charged leptons are identified with their mass eigenstates. Namely,

$$M_\nu = \begin{pmatrix} \langle m \rangle_{ee} & \langle m \rangle_{e\mu} & \langle m \rangle_{e\tau} \\ \langle m \rangle_{e\mu} & \langle m \rangle_{\mu\mu} & \langle m \rangle_{\mu\tau} \\ \langle m \rangle_{e\tau} & \langle m \rangle_{\mu\tau} & \langle m \rangle_{\tau\tau} \end{pmatrix}, \quad (26)$$

where $\langle m \rangle_{\beta\alpha} = \langle m \rangle_{\alpha\beta}$ has been taken into account. In the standard parametrization of U , we have

$$\begin{aligned} \langle m \rangle_{ee} &= m_1 c_{12}^2 c_{13}^2 e^{2i\rho} + m_2 s_{12}^2 c_{13}^2 e^{2i\sigma} + m_3 s_{13}^2 e^{-2i\delta}, \\ \langle m \rangle_{\mu\mu} &= m_1 \left(s_{12} c_{23} + c_{12} s_{13} s_{23} e^{i\delta} \right)^2 e^{2i\rho} + m_2 \left(c_{12} c_{23} - s_{12} s_{13} s_{23} e^{i\delta} \right)^2 e^{2i\sigma} + m_3 c_{13}^2 s_{23}^2, \\ \langle m \rangle_{\tau\tau} &= m_1 \left(s_{12} s_{23} - c_{12} s_{13} c_{23} e^{i\delta} \right)^2 e^{2i\rho} + m_2 \left(c_{12} s_{23} + s_{12} s_{13} c_{23} e^{i\delta} \right)^2 e^{2i\sigma} + m_3 c_{13}^2 c_{23}^2, \\ \langle m \rangle_{e\mu} &= -m_1 c_{12} c_{13} \left(s_{12} c_{23} + c_{12} s_{13} s_{23} e^{i\delta} \right) e^{2i\rho} + m_2 s_{12} c_{13} \left(c_{23} c_{12} - s_{12} s_{13} s_{23} e^{i\delta} \right) e^{2i\sigma} \\ &\quad + m_3 c_{13} s_{13} s_{23} e^{-i\delta}, \\ \langle m \rangle_{e\tau} &= +m_1 c_{12} c_{13} \left(s_{12} s_{23} - c_{12} s_{13} c_{23} e^{i\delta} \right) e^{2i\rho} - m_2 s_{12} c_{13} \left(c_{12} s_{23} + s_{12} s_{13} c_{23} e^{i\delta} \right) e^{2i\sigma} \\ &\quad + m_3 c_{13} s_{13} c_{23} e^{-i\delta}, \\ \langle m \rangle_{\mu\tau} &= -m_1 \left(s_{12} s_{23} - c_{12} s_{13} c_{23} e^{i\delta} \right) \left(c_{23} s_{12} + c_{12} s_{13} s_{23} e^{i\delta} \right) e^{2i\rho} \\ &\quad - m_2 \left(c_{12} s_{23} + s_{12} s_{13} c_{23} e^{i\delta} \right) \left(c_{12} c_{23} - s_{12} s_{13} s_{23} e^{i\delta} \right) e^{2i\sigma} + m_3 c_{13}^2 c_{23} s_{23}. \end{aligned} \quad (27)$$

We see that a measurement of the three CP-violating phases is absolutely necessary in order to fully reconstruct the neutrino mass matrix M_ν . Without the information on ρ and σ , it would be impossible to model-independently look into the structure of M_ν via a bottom-up approach. On the other hand, a predictive model of lepton flavors should be able to specify the texture of M_ν via a top-down approach, such that its predictions can be experimentally tested.

Note that $|\langle m \rangle_\alpha|^2$ in Eq. (10) can be related to $\langle m \rangle_{\alpha\beta}$ as follows:

$$\sum_\beta |\langle m \rangle_{\alpha\beta}|^2 = |\langle m \rangle_\alpha|^2 = \sum_i m_i^2 |U_{\alpha i}|^2, \quad (28)$$

It is obvious that all the $|\langle m \rangle_\alpha|^2$ do not contain any information about the Majorana phases ρ and σ , but they may depend on the ‘‘Dirac’’ phase δ . Furthermore, we have

$$\sum_\alpha |\langle m \rangle_\alpha|^2 = \sum_i m_i^2 = 3m_1^2 + \Delta m_{21}^2 + \Delta m_{31}^2 = 3m_3^2 - \Delta m_{21}^2 - 2\Delta m_{32}^2, \quad (29)$$

where $\Delta m_{ij}^2 \equiv m_i^2 - m_j^2$ (for $i, j = 1, 2, 3$). A global analysis of current neutrino oscillation data has given $\Delta m_{21}^2 \simeq 7.50 \times 10^{-5} \text{ eV}^2$ and $\Delta m_{31}^2 \simeq 2.473 \times 10^{-3} \text{ eV}^2$ (normal neutrino mass hierarchy) or $\Delta m_{32}^2 \simeq -2.427 \times 10^{-3} \text{ eV}^2$ (inverted neutrino mass hierarchy) [15]. Therefore,

$$\begin{aligned} \text{Normal hierarchy :} & \quad \sum_i m_i^2 \geq \Delta m_{21}^2 + \Delta m_{31}^2 \simeq 2.55 \times 10^{-3} \text{ eV}^2, \\ \text{Inverted hierarchy :} & \quad \sum_i m_i^2 \geq -\Delta m_{21}^2 - 2\Delta m_{32}^2 \simeq 4.78 \times 10^{-3} \text{ eV}^2, \end{aligned} \quad (30)$$

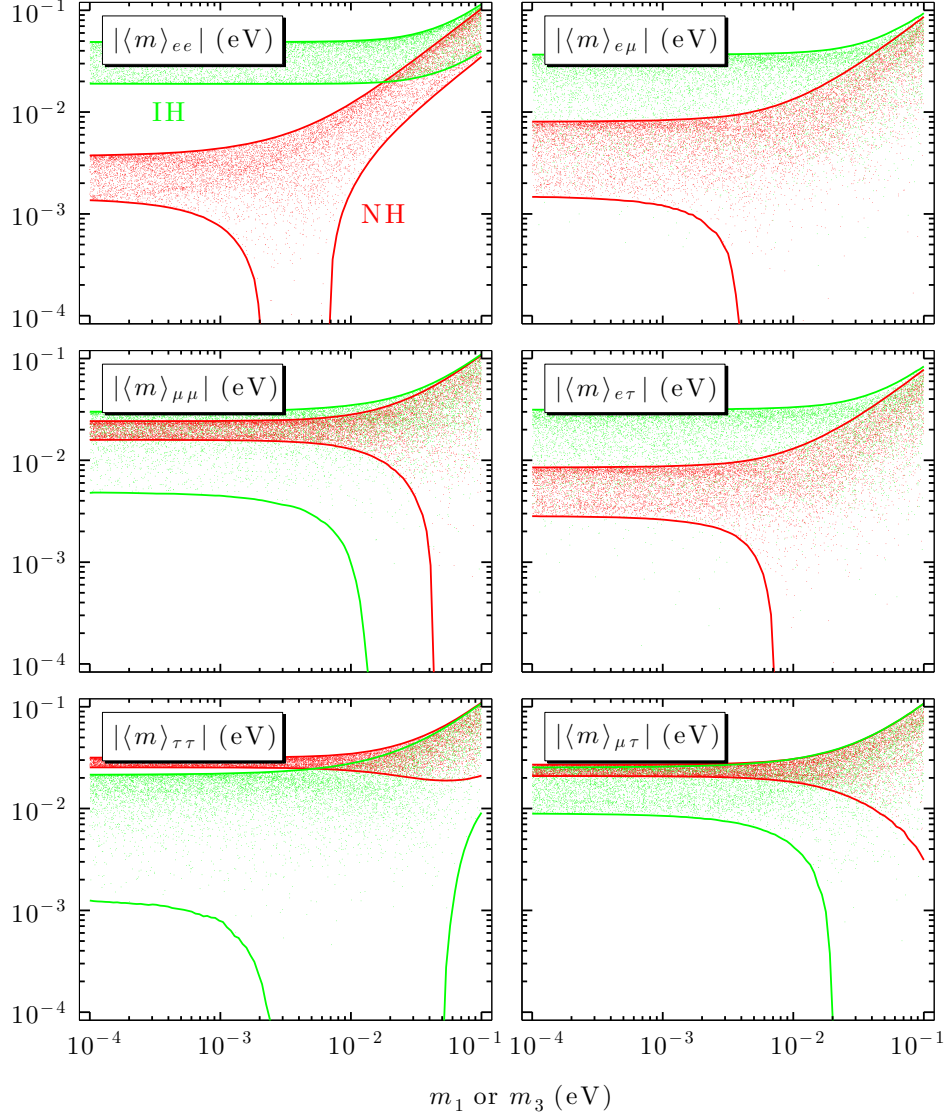


Figure 4: The profiles of $|\langle m \rangle_{\alpha\beta}|$ versus the lightest neutrino mass m_1 (normal hierarchy or NH: red region) or m_3 (inverted hierarchy or IH: green region).

where the lower bounds correspond to $m_1 = 0$ (normal hierarchy) and $m_3 = 0$ (inverted hierarchy), respectively. On the other hand, the sum of the three neutrino masses can also be written as

$$\begin{aligned}
 \sum_i m_i &= m_1 + \sqrt{m_1^2 + \Delta m_{21}^2} + \sqrt{m_1^2 + \Delta m_{31}^2} \\
 &= m_3 + \sqrt{m_3^2 - \Delta m_{32}^2} + \sqrt{m_3^2 - \Delta m_{32}^2 - \Delta m_{21}^2} .
 \end{aligned} \tag{31}$$

This sum has well been constrained thanks to the recent WMAP [18] and PLANCK [19] data, and its upper bound is about 0.23 eV at the 95% confidence level [19]. One may then obtain the allowed range of the lightest neutrino mass by using the above inputs: $0 \lesssim m_1 \lesssim 0.071$ eV in the normal hierarchy; or $0 \lesssim m_3 \lesssim 0.065$ eV in the inverted hierarchy.

Figure 4 illustrate the profiles of six $|\langle m \rangle_{\alpha\beta}|$. Our inputs are $\theta_{12} \simeq 33.4^\circ$, $\theta_{13} \simeq 8.66^\circ$ and $\theta_{23} \simeq 40.0^\circ$; $\Delta m_{21}^2 \simeq 7.50 \times 10^{-5}$ eV² and $\Delta m_{31}^2 \simeq 2.473 \times 10^{-3}$ eV² (normal hierarchy) or $\Delta m_{32}^2 \simeq -2.427 \times 10^{-3}$ eV²

(inverted hierarchy) [15]. As for the three unknown phase parameters, we allow the ‘‘Dirac’’ phase δ to randomly vary between 0° and 360° , and allow the Majorana phases ρ and σ to randomly vary between 0° and 180° . We plot the results of $|\langle m \rangle_{\alpha\beta}|$ versus the lightest neutrino mass in Figure 4 by allowing the latter to vary from 10^{-4} eV to 10^{-1} eV, where the upper bound is set by taking account of the recent PLANCK data [19]. To understand our numerical results, we have also made some analytical approximations for $\langle m \rangle_{\alpha\beta}$ in Appendix B. Some discussions are in order.

- Given the normal neutrino mass hierarchy, most of the random points of $|\langle m \rangle_{\mu\mu}|$, $|\langle m \rangle_{\tau\tau}|$, $|\langle m \rangle_{\mu\tau}|$ are located in the region of 10^{-2} eV to 10^{-1} eV. This observation is also true for all the $|\langle m \rangle_{\alpha\beta}|$ in the inverted hierarchy. Such results are compatible with the analytical approximations made in Appendix B. The point is that the relevant $|\langle m \rangle_{\alpha\beta}|$ are dominated by $\sqrt{|\Delta m_{31}^2|} \simeq \sqrt{|\Delta m_{32}^2|} \simeq 0.05$ eV when the lightest neutrino mass is sufficiently small, and all the $|\langle m \rangle_{\alpha\beta}|$ approach $m_1 \simeq m_2 \simeq m_3 > 0.05$ eV for a nearly degenerate neutrino mass spectrum.
- The random points of $|\langle m \rangle_{ee}|$, $|\langle m \rangle_{e\mu}|$ and $|\langle m \rangle_{e\tau}|$ in the normal hierarchy are most likely to lie in the region of 10^{-3} eV to 10^{-2} eV, especially when $m_1^2 \ll \Delta m_{31}^2$. Their magnitudes are in general smaller than those in the inverted hierarchy. The reason is simply that $|\langle m \rangle_{ee}| \sim \sqrt{\Delta m_{21}^2} s_{12}^2 \simeq 2.6 \times 10^{-3}$ eV and $|\langle m \rangle_{e\mu}| \sim |\langle m \rangle_{e\tau}| \sim \sqrt{\Delta m_{31}^2} s_{13} \simeq 7.5 \times 10^{-3}$ eV hold in the normal hierarchy, while in the inverted hierarchy the dominant masses $m_1 \simeq m_2 \simeq \sqrt{-\Delta m_{32}^2}$ do not undergo this s_{13} suppression (see Appendix B).
- In the limit where the lightest neutrino mass approaches zero or much smaller than $\sqrt{\Delta m_{21}^2}$, the allowed region of $|\langle m \rangle_{\alpha\beta}|$ in the normal hierarchy is narrower than that in the inverted hierarchy, as shown in Figure 4, where the only exception is $|\langle m \rangle_{ee}|$. The reason can be seen from Eqs. (49)—(52) in Appendix B: the dominant term of each $|\langle m \rangle_{\alpha\beta}|$ (for $\alpha\beta \neq ee$) is proportional to $\sqrt{\Delta m_{31}^2}$ and its uncertainty is associated with $\sqrt{\Delta m_{21}^2}$ in the normal hierarchy, while the uncertainty of the same effective mass term in the inverted hierarchy does not undergo this suppression. Because the two terms of $\langle m \rangle_{ee}$ in Eq. (49) are almost comparable in magnitude, its magnitude involves a relatively large uncertainty in the normal hierarchy as in the inverted hierarchy.
- In the $m_1 \simeq m_2 \simeq m_3$ limit, which is guaranteed if the lightest neutrino mass is larger or much larger than $\sqrt{|\Delta m_{31}^2|} \simeq \sqrt{|\Delta m_{32}^2|} \simeq 0.05$ eV, the $|\langle m \rangle_{\alpha\beta}|$ in both normal and inverted hierarchies should have the same bounds. This is because the m_i can be factored out from the expression of each $|\langle m \rangle_{\alpha\beta}|$, making the latter insensitive to the ordering of the three masses. Such a feature has essentially been reflected in Figure 4 (see the limit of $m_1 \rightarrow 0.1$ eV or $m_3 \rightarrow 0.1$ eV), and it will become more obvious if m_1 (or m_3) runs to much larger values, such as 0.2 eV or even 0.5 eV. See also Appendix B for some relevant analytical approximations in this case.
- For some values of the lightest neutrino mass, $|\langle m \rangle_{\alpha\beta}| = 0$ is always allowed, as shown in Figure 4, either in the normal hierarchy (e.g., $|\langle m \rangle_{ee}| = 0$ [20]) or in the inverted hierarchy (e.g., $|\langle m \rangle_{\tau\tau}| = 0$), or in both of them (e.g., $|\langle m \rangle_{e\mu}| = 0$). This kind of *texture zeros* implies that significant cancellations can happen in $|\langle m \rangle_{\alpha\beta}|$ due to the unknown CP-violating phases [20, 21]. For instance, $\rho = \sigma$ may lead to $|\langle m \rangle_{e\mu}| \simeq |\langle m \rangle_{e\tau}| \simeq 0$ when the three neutrino masses are nearly degenerate, as one can see from Eq. (53) in Appendix B. Fortunately, it is impossible for all the $|\langle m \rangle_{\alpha\beta}|$ to be simultaneously vanishing or highly suppressed, no matter what values m_1 or m_3 may take. Unfortunately, current experimental techniques only allow us to constrain $|\langle m \rangle_{ee}|$ via a careful measurement of the $0\nu\beta\beta$ decay [8].

Table 2: The branching ratios of the LNV $H^+ \rightarrow \ell_\alpha^+ \bar{\nu}$ decay modes in four different neutrino mass hierarchies, where $\delta = 90^\circ$ has been assumed.

Normal hierarchy	$m_1 = 0$	$m_1 = 0.1 \text{ eV}$
$\mathcal{B}(H^+ \rightarrow e^+ \bar{\nu})$	0.03	0.31
$\mathcal{B}(H^+ \rightarrow \mu^+ \bar{\nu})$	0.41	0.34
$\mathcal{B}(H^+ \rightarrow \tau^+ \bar{\nu})$	0.56	0.35
Inverted hierarchy	$m_3 = 0$	$m_3 = 0.1 \text{ eV}$
$\mathcal{B}(H^+ \rightarrow e^+ \bar{\nu})$	0.21	0.32
$\mathcal{B}(H^+ \rightarrow \mu^+ \bar{\nu})$	0.30	0.33
$\mathcal{B}(H^+ \rightarrow \tau^+ \bar{\nu})$	0.49	0.35

Taking the upper bound of the sum of three neutrino masses as set by the recent PLANCK data (i.e., $m_1 + m_2 + m_3 < 0.23 \text{ eV}$ at the 95% confidence level [19]), we may obtain the upper bounds on all the $|\langle m \rangle_{\alpha\beta}|$ from our numerical calculations:

$$\begin{aligned}
 |\langle m \rangle_{ee}| &\lesssim 0.072 \text{ eV}, & |\langle m \rangle_{\mu\mu}| &\lesssim 0.077 \text{ eV}, & |\langle m \rangle_{\tau\tau}| &\lesssim 0.080 \text{ eV}, \\
 |\langle m \rangle_{e\mu}| &\lesssim 0.060 \text{ eV}, & |\langle m \rangle_{e\tau}| &\lesssim 0.055 \text{ eV}, & |\langle m \rangle_{\mu\tau}| &\lesssim 0.078 \text{ eV},
 \end{aligned}$$

for the normal neutrino mass hierarchy; and

$$\begin{aligned}
 |\langle m \rangle_{ee}| &\lesssim 0.082 \text{ eV}, & |\langle m \rangle_{\mu\mu}| &\lesssim 0.075 \text{ eV}, & |\langle m \rangle_{\tau\tau}| &\lesssim 0.072 \text{ eV}, \\
 |\langle m \rangle_{e\mu}| &\lesssim 0.065 \text{ eV}, & |\langle m \rangle_{e\tau}| &\lesssim 0.058 \text{ eV}, & |\langle m \rangle_{\mu\tau}| &\lesssim 0.072 \text{ eV},
 \end{aligned}$$

for the inverted neutrino mass hierarchy.

3.3 $H^{++} \rightarrow \ell_\alpha^+ \ell_\beta^+$ and $H^+ \rightarrow \ell_\alpha^+ \bar{\nu}$ decays

There exist a number of viable mechanisms which can explain why the neutrino masses are naturally tiny [22]. Among them, the type-II seesaw mechanism [7] is of particular interest because it can keep the unitarity of the PMNS matrix U unviolated and lead to very rich collider phenomenology [23]. The latter includes the LNV decay modes $H^{++} \rightarrow \ell_\alpha^+ \ell_\beta^+$ and $H^+ \rightarrow \ell_\alpha^+ \bar{\nu}$. Their branching ratios are

$$\mathcal{B}(H^{++} \rightarrow \ell_\alpha^+ \ell_\beta^+) \equiv \frac{\Gamma(H^{++} \rightarrow \ell_\alpha^+ \ell_\beta^+)}{\sum_\alpha \sum_\beta \Gamma(H^{++} \rightarrow \ell_\alpha^+ \ell_\beta^+)} = \frac{2}{(1 + \delta_{\alpha\beta})} \cdot \frac{|\langle m \rangle_{\alpha\beta}|^2}{\sum_i m_i^2}, \quad (32)$$

and

$$\mathcal{B}(H^+ \rightarrow \ell_\alpha^+ \bar{\nu}) \equiv \frac{\sum_\beta \Gamma(H^+ \rightarrow \ell_\alpha^+ \bar{\nu}_\beta)}{\sum_\alpha \sum_\beta \Gamma(H^+ \rightarrow \ell_\alpha^+ \bar{\nu}_\beta)} = \frac{|\langle m \rangle_\alpha|^2}{\sum_i m_i^2}, \quad (33)$$

respectively, where the Greek subscripts run over e , μ and τ . Taking account of Eq. (28), we see that $\mathcal{B}(H^+ \rightarrow \ell_\alpha^+ \bar{\nu})$ only depends on the ‘‘Dirac’’ phase δ , while $\mathcal{B}(H^{++} \rightarrow \ell_\alpha^+ \ell_\beta^+)$ is sensitive to all the three

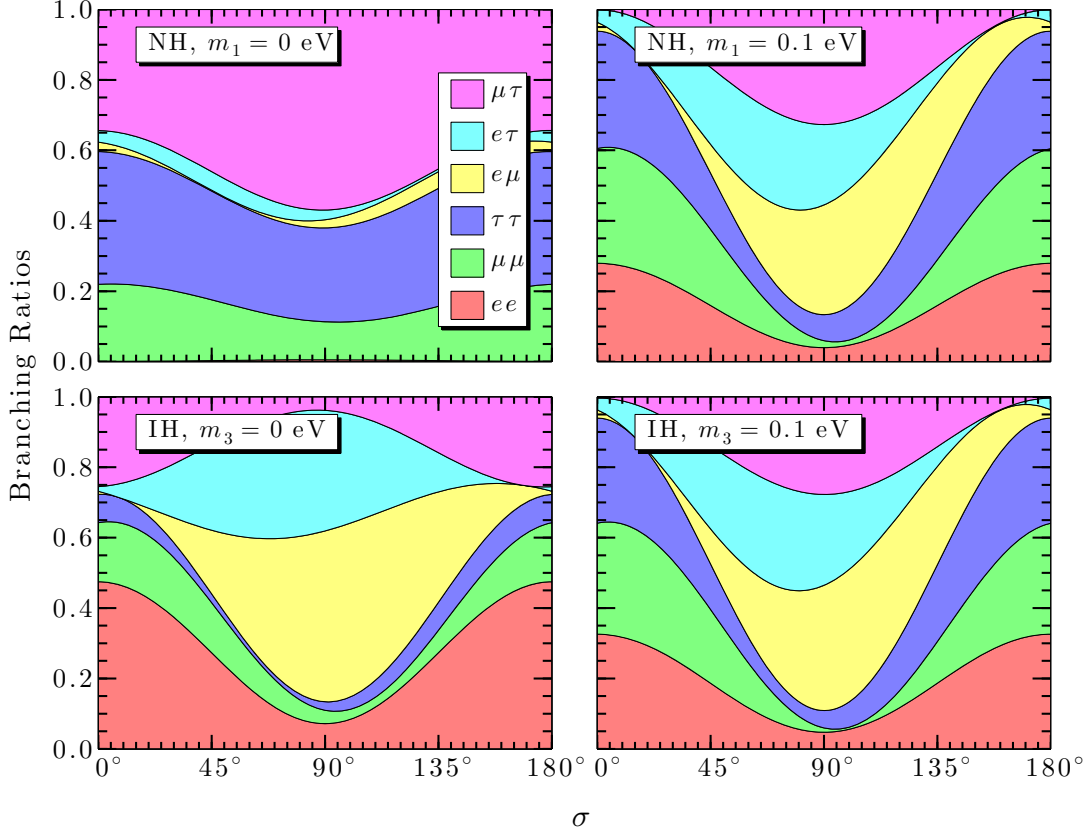


Figure 5: The branching ratios of the LNV $H^{++} \rightarrow \ell_\alpha^+ \ell_\beta^+$ decays as functions of the Majorana phase σ , where $\rho = 0^\circ$ and $\delta = 90^\circ$ are taken. Four typical cases of the neutrino mass spectrum are considered: the normal hierarchy (NH) with $m_1 = 0$ or 0.1 eV; and the inverted hierarchy with $m_3 = 0$ or 0.1 eV.

CP-violating phases. These interesting LNV decay modes deserve a reexamination because the previous works [23, 24] were more or less subject to the assumption of vanishing or very small θ_{13} , making the role of δ unimportant. In view of the experimental fact that θ_{13} is not that small [10, 11], we update the numerical analysis of $\mathcal{B}(H^+ \rightarrow \ell_\alpha^+ \bar{\nu})$ and $\mathcal{B}(H^{++} \rightarrow \ell_\alpha^+ \ell_\beta^+)$ by taking the same inputs as above. Our results are presented in Table 2 and Figures 5–7, respectively.

We first look at the branching ratios $\mathcal{B}(H^+ \rightarrow \ell_\alpha^+ \bar{\nu})$, whose magnitudes are governed by

$$|\langle m \rangle_\alpha|^2 = \sum_i m_i^2 |U_{\alpha i}|^2 = m_1^2 (1 - |U_{\alpha 3}|^2) + m_3^2 |U_{\alpha 3}|^2 + \Delta m_{21}^2 |U_{\alpha 2}|^2, \quad (34)$$

in which only the $U_{\alpha 2}$ elements (for $\alpha = e, \mu, \tau$) contain δ , as shown in Eq. (1). Hence the contributions of δ to $|\langle m \rangle_\alpha|$ and $\mathcal{B}(H^+ \rightarrow \ell_\alpha^+ \bar{\nu})$ are suppressed not only by the smallness of θ_{13} but also by the smallness of Δm_{21}^2 . In particular, $\mathcal{B}(H^+ \rightarrow e^+ \bar{\nu})$ is exactly independent of δ . These LNV decay modes are actually not useful to probe the “Dirac” phase δ . We use the typical inputs of three neutrino mixing angles and two neutrino mass-squared differences given above to calculate $\mathcal{B}(H^+ \rightarrow \ell_\alpha^+ \bar{\nu})$, and list the numerical results in Table 2, where $\delta = 90^\circ$ has been assumed. When varying δ from 0° to 360° , we find that the δ -induced uncertainties of all the branching ratios are lower than 1%.

Now let us turn to the branching ratios of the LNV $H^{++} \rightarrow \ell_\alpha^+ \ell_\beta^+$ decays. We take $(\rho, \delta) = (0^\circ, 90^\circ)$, $(45^\circ, 0^\circ)$ and $(45^\circ, 90^\circ)$ to show how $\mathcal{B}(H^{++} \rightarrow \ell_\alpha^+ \ell_\beta^+)$ changes with σ in Figures 5–7, respectively. Both the normal hierarchy with $m_1 = 0$ (or 0.1 eV) and the inverted hierarchy with $m_3 = 0$ (or 0.1 eV)

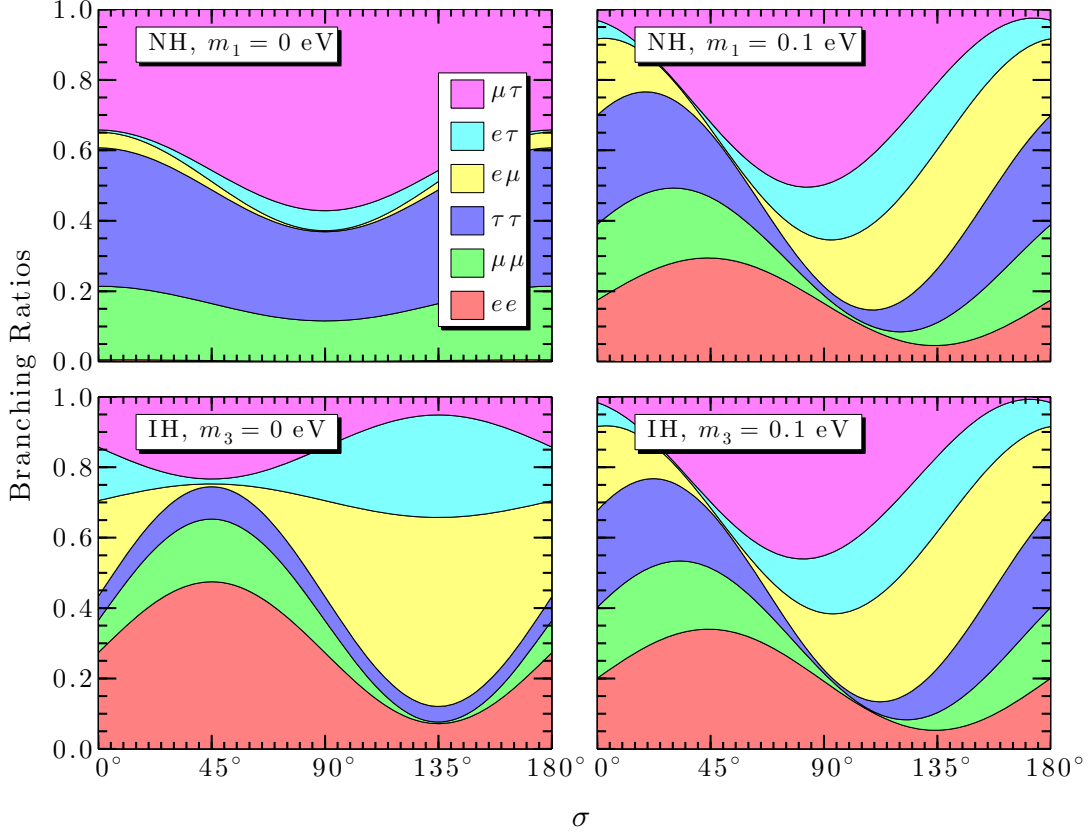


Figure 6: The branching ratios of the LNV $H^{++} \rightarrow \ell_{\alpha}^{+} \ell_{\beta}^{+}$ decays as functions of the Majorana phase σ , where $\rho = 45^{\circ}$ and $\delta = 0^{\circ}$ are taken. Four typical cases of the neutrino mass spectrum are considered: the normal hierarchy (NH) with $m_1 = 0$ or 0.1 eV; and the inverted hierarchy with $m_3 = 0$ or 0.1 eV.

are considered in each of the figures. Some discussions are in order.

- The sum of the six independent branching ratios is equal to one, as guaranteed by Eq. (32) and the unitarity of the PMNS matrix U . This point can be clearly seen in each figure, which is exactly saturated by six different branching ratios.
- In the normal neutrino mass hierarchy with $m_1 = 0$, the magnitude of $\langle m \rangle_{ee}$ is highly suppressed, and thus $\mathcal{B}(H^{++} \rightarrow e^{+}e^{+}) \simeq 0$. In this special case $\mathcal{B}(H^{++} \rightarrow e^{+}\mu^{+})$ and $\mathcal{B}(H^{++} \rightarrow e^{+}\tau^{+})$ are also very small. In the inverted neutrino mass hierarchy with $m_3 = 0$, the $H^{++} \rightarrow \tau^{+}\tau^{+}$ channel is strongly suppressed.
- The Majorana phases ρ and σ play an important role in all the six LNV decay modes. They may significantly affect the branching ratio of each process, making themselves easier to be detected. Given some specific values of ρ and δ , each $\mathcal{B}(H^{++} \rightarrow \ell_{\alpha}^{+}\ell_{\beta}^{+})$ changes as a simple trigonometric function of σ . When ρ changes from one given value to another, the profile of the branching ratio of each decay mode will more or less shift and deform.
- In some cases, the three CP-violating phases may give rise to large cancellations in $\langle m \rangle_{\alpha\beta}$, making some of the LNV decay modes significantly suppressed. In the $(\rho, \sigma) = (0^{\circ}, 90^{\circ})$ case, for example, the $H^{++} \rightarrow e^{+}e^{+}$, $H^{++} \rightarrow \mu^{+}\mu^{+}$ and $H^{++} \rightarrow \tau^{+}\tau^{+}$ channels are somewhat suppressed when the lightest neutrino mass is about 0.1 eV. It is therefore difficult to detect them.

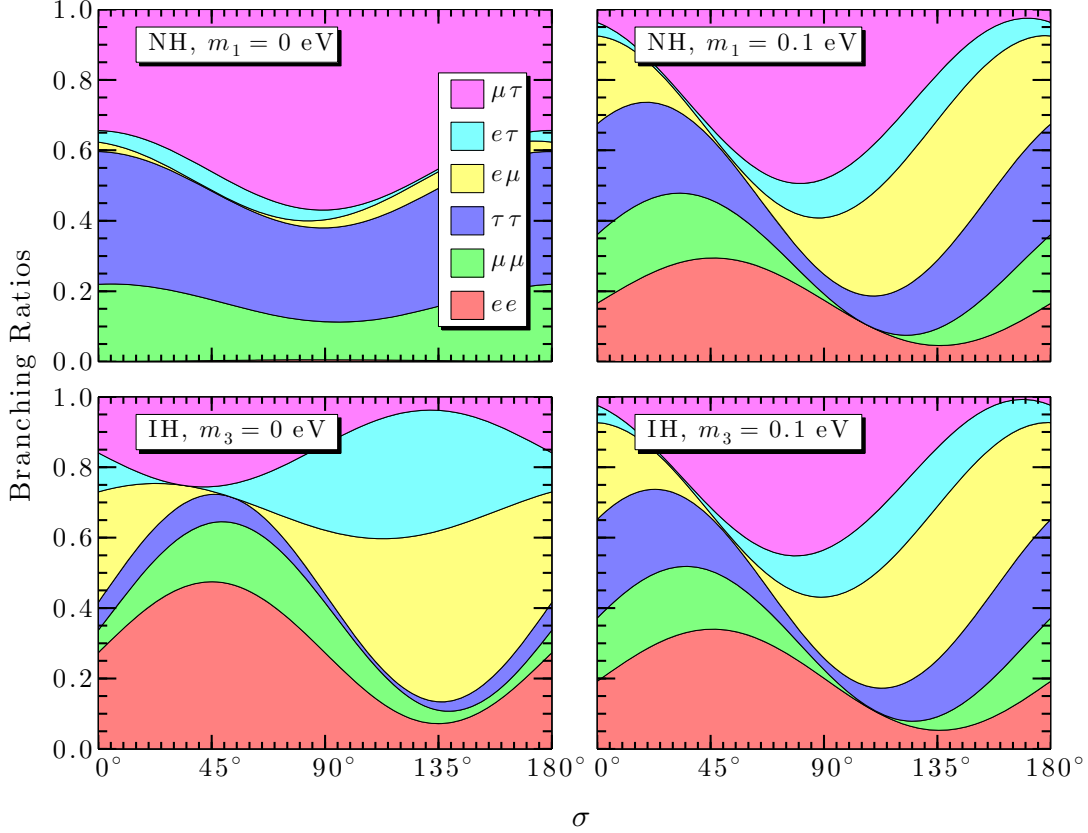


Figure 7: The branching ratios of the LNV $H^{++} \rightarrow \ell_\alpha^+ \ell_\beta^+$ decays as functions of the Majorana phase σ , where $\rho = 45^\circ$ and $\delta = 90^\circ$ are taken. Four typical cases of the neutrino mass spectrum are considered: the normal hierarchy (NH) with $m_1 = 0$ or 0.1 eV; and the inverted hierarchy with $m_3 = 0$ or 0.1 eV.

- The “Dirac” phase δ , whose effect is always suppressed by the smallness of θ_{13} , has relatively small influence on the branching ratios of the LNV $H^{++} \rightarrow \ell_\alpha^+ \ell_\beta^+$ decays. A comparison between Figures 6 and 7 indicates that the relevant numerical results do not change much when δ changes from 0° to 90° . But the interplay of δ and ρ (or σ) is sometimes important.
- The branching ratios in the normal hierarchy with $m_1 = 0.1$ eV and in the inverted hierarchy with $m_3 = 0.1$ eV are almost the same. The reason is simply that these two cases belong to the nearly degenerate mass hierarchy (i.e., $m_1 \simeq m_2 \simeq m_3$).

The behaviors of $\mathcal{B}(H^{++} \rightarrow \ell_\alpha^+ \ell_\beta^+)$ changing with the lightest neutrino mass are essentially similar to those of $|\langle m \rangle_{\alpha\beta}|$ shown in Figure 4, and hence we do not go into detail in this connection.

4 CP violation in neutrino-antineutrino oscillations

In this section we carry out a detailed analysis of all the possible CP-violating asymmetries $\mathcal{A}_{\alpha\beta}$ between $\nu_\alpha \rightarrow \bar{\nu}_\beta$ and $\bar{\nu}_\alpha \rightarrow \nu_\beta$ oscillations. The generic expression of $\mathcal{A}_{\alpha\beta}$ has been given in Eq. (12). Because of the fact $|\Delta m_{31}^2| \simeq |\Delta m_{32}^2| \simeq 32\Delta m_{21}^2$, there may exist two oscillating regions dominated respectively by Δm_{21}^2 and Δm_{31}^2 . Let us make some analytical approximations for each of these two regions.

- The oscillating region dominated by Δm_{31}^2 (or Δm_{32}^2), in which $|\phi_{31}| \sim \mathcal{O}(1)$ and $\phi_{21} \ll \mathcal{O}(1)$. In

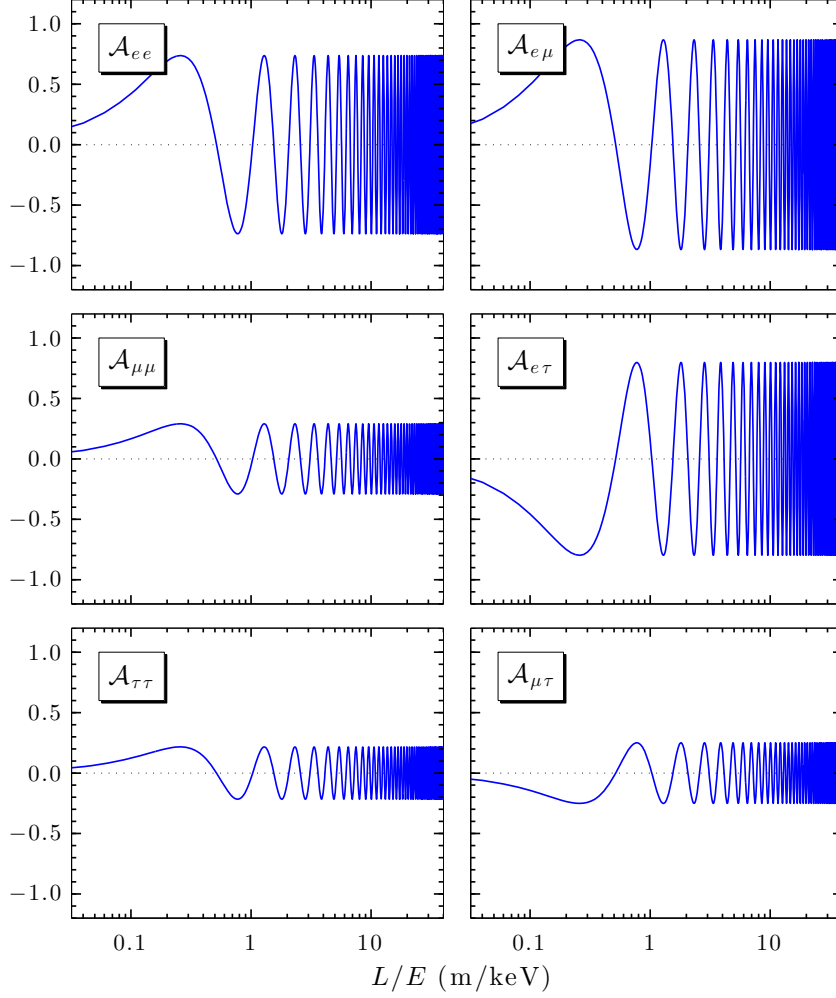


Figure 8: The CP-violating asymmetries $\mathcal{A}_{\alpha\beta}$ versus L/E in the normal neutrino mass hierarchy with $m_1 = 0$, $\delta = 0^\circ$ and $\sigma = 45^\circ$.

the neglect of the Δm_{21}^2 -driven contributions, Eq. (12) approximates to

$$\mathcal{A}_{\alpha\beta}^{31} \simeq \frac{2m_3 (m_1 \mathcal{V}_{\alpha\beta}^{13} + m_2 \mathcal{V}_{\alpha\beta}^{23}) \sin 2\phi_{31}}{|\langle m \rangle_{\alpha\beta}|^2 - 4m_3 (m_1 \mathcal{C}_{\alpha\beta}^{13} + m_2 \mathcal{C}_{\alpha\beta}^{23}) \sin^2 \phi_{31}}, \quad (35)$$

where $\phi_{32} \simeq \phi_{31}$ has been taken into account.

- The oscillating region dominated by Δm_{21}^2 , in which $\phi_{21} \sim \mathcal{O}(1)$ and $|\phi_{31}| \gg \mathcal{O}(1)$. Hence the $\sin^2 \phi_{31}$ and $\sin^2 \phi_{32}$ terms in Eq. (3) oscillate too fast and each of them averages out to 1/2, while the $\sin 2\phi_{31}$ and $\sin 2\phi_{32}$ terms average out to zero. In this case Eq. (12) approximates to

$$\mathcal{A}_{\alpha\beta}^{21} \simeq \frac{2m_1 m_2 \mathcal{V}_{\alpha\beta}^{12} \sin 2\phi_{21}}{|\langle m \rangle_{\alpha\beta}|^2 - 2m_3 (m_1 \mathcal{C}_{\alpha\beta}^{13} + m_2 \mathcal{C}_{\alpha\beta}^{23}) - 4m_1 m_2 \mathcal{C}_{\alpha\beta}^{12} \sin^2 \phi_{21}}. \quad (36)$$

Our numerical calculations will be based on the exact formula given in Eq. (12), but the approximations made in Eqs. (35) and (36) are helpful to understand the quantitative behaviors of $\mathcal{A}_{\alpha\beta}^{ij}$. To reveal the salient features of all the $\mathcal{A}_{\alpha\beta}^{ij}$, we are going to examine their dependence on the ratio L/E , the three CP-violating phases and the absolute neutrino mass in Figures 8–16.

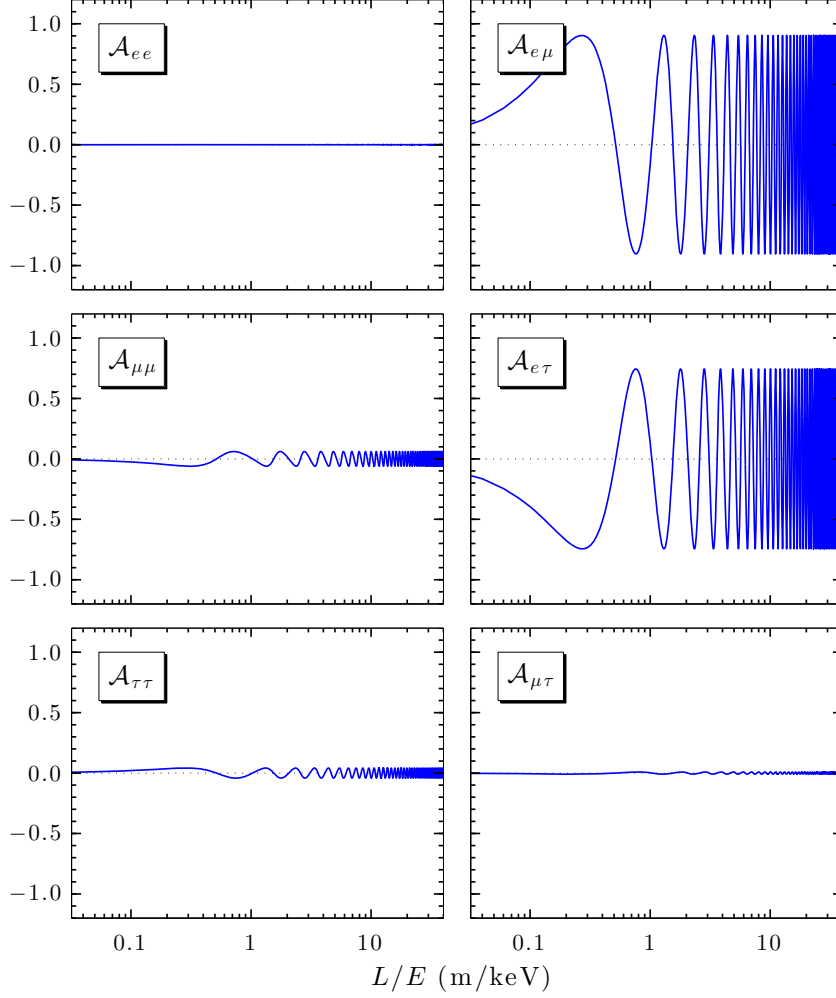


Figure 9: The CP-violating asymmetries $\mathcal{A}_{\alpha\beta}$ versus L/E in the normal neutrino mass hierarchy with $m_1 = 0$, $\delta = 90^\circ$ and $\sigma = 0^\circ$.

4.1 The dependence of $\mathcal{A}_{\alpha\beta}^{ij}$ on L/E and (δ, ρ, σ)

Let us consider three special cases for the neutrino mass spectrum, in which the expressions of $\mathcal{A}_{\alpha\beta}^{ij}$ can be more or less simplified, to illustrate their dependence on the ratio L/E and the phases δ , ρ and σ .

(A) The normal neutrino mass hierarchy with $m_1 = 0$. In this case we obtain $m_2 = \sqrt{\Delta m_{21}^2} \simeq 8.66 \times 10^{-3}$ eV and $m_3 = \sqrt{\Delta m_{31}^2} \simeq 4.97 \times 10^{-2}$ eV. Eq. (12) is now simplified to

$$\mathcal{A}_{\alpha\beta} = \frac{2\mathcal{V}_{\alpha\beta}^{23} \sin 2\phi_{31}}{\sqrt{\frac{\Delta m_{21}^2}{\Delta m_{31}^2}} \mathcal{C}_{\alpha\beta}^{22} + \sqrt{\frac{\Delta m_{31}^2}{\Delta m_{21}^2}} \mathcal{C}_{\alpha\beta}^{33} + 2\mathcal{C}_{\alpha\beta}^{23} \cos 2\phi_{31}}. \quad (37)$$

Note that the Majorana phase ρ does not contribute to $\mathcal{A}_{\alpha\beta}$ in the $m_1 = 0$ limit [6]. This point can also be seen in Eq. (37): both $\mathcal{C}_{\alpha\beta}^{23}$ and $\mathcal{V}_{\alpha\beta}^{23}$ do not contain ρ , nor do $\mathcal{C}_{\alpha\beta}^{22}$ and $\mathcal{C}_{\alpha\beta}^{33}$. For simplicity, we choose $(\delta, \sigma) = (0^\circ, 45^\circ)$, $(90^\circ, 0^\circ)$ and $(90^\circ, 45^\circ)$ to calculate all the six independent $\mathcal{A}_{\alpha\beta}^{ij}$, and show their numerical results in Figures 8–10. Some comments are in order.

- Figure 8 illustrates that significant CP-violating effects can show up in neutrino-antineutrino oscillations even though the “Dirac” phase δ vanishes. They arise from the Majorana phase σ ,

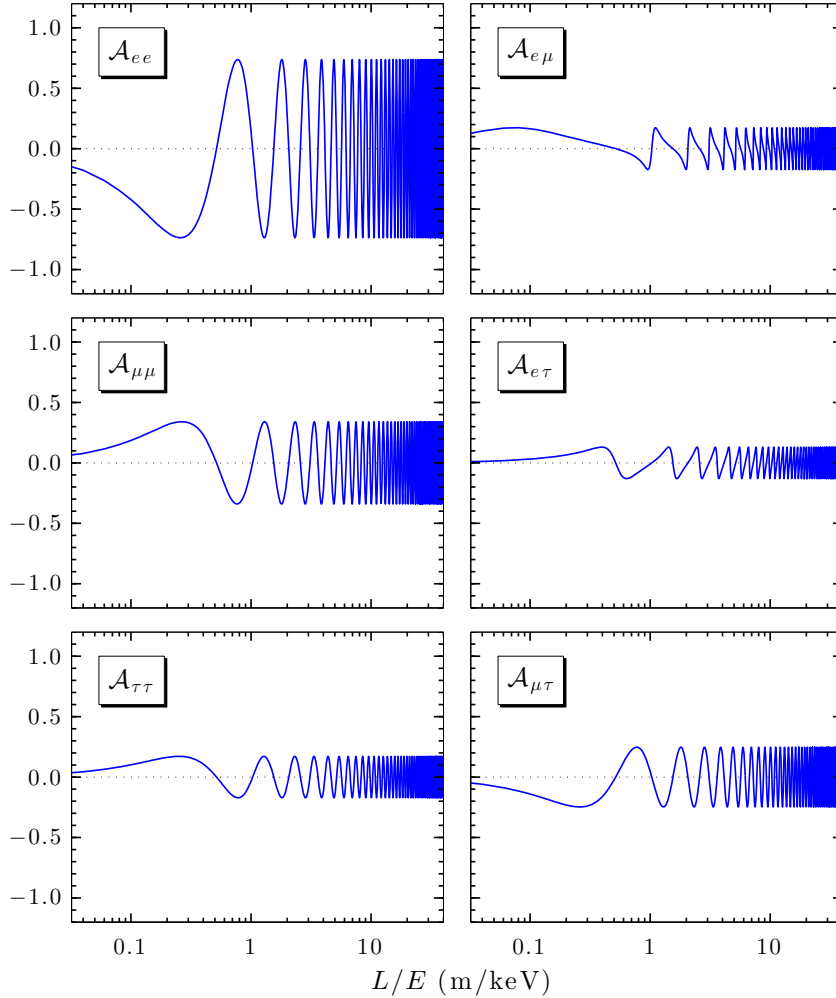


Figure 10: The CP-violating asymmetries $\mathcal{A}_{\alpha\beta}$ versus L/E in the normal neutrino mass hierarchy with $m_1 = 0$, $\delta = 90^\circ$ and $\sigma = 45^\circ$.

which has nothing to do with CP and T violation in normal neutrino-neutrino or antineutrino-antineutrino oscillations. We have taken $\rho = 45^\circ$ to maximize each CP-violating term in $\mathcal{A}_{\alpha\beta}$, where ρ and σ enter in the form of 2ρ and 2σ , as one can see from Eqs. (19)–(24)⁴.

- Figure 9 illustrates the nontrivial role of δ in generating CP or T violation in neutrino-antineutrino oscillations. Hence it is intrinsically a Majorana phase. In particular, $\delta = 90^\circ$ (the most favored value to enhance the magnitude of \mathcal{J}) can lead to large CP-violating asymmetries between $\nu_e \rightarrow \bar{\nu}_\mu$ and $\bar{\nu}_e \rightarrow \nu_\mu$ oscillations and between $\nu_e \rightarrow \bar{\nu}_\tau$ and $\bar{\nu}_e \rightarrow \nu_\tau$ oscillations. But the other four CP-violating asymmetries are quite insensitive to δ in this case.
- A comparison between Figures 9 and 10 tells us again how important the Majorana phase σ is in producing CP and T violation. The interplay of δ and σ can be either positive or negative, depending on their explicit values. In order to determine all the three CP-violating phases, one has to try to measure the CP-violating effects in as many channels as possible. Fortunately, not all the channels are strongly suppressed in most cases, unless δ , ρ and σ themselves are too small

⁴One may redefine $\rho \equiv \rho'/2$ and $\sigma \equiv \sigma'/2$ in the PMNS matrix U , so as to eliminate the factor 2 from Eqs. (19)–(24).

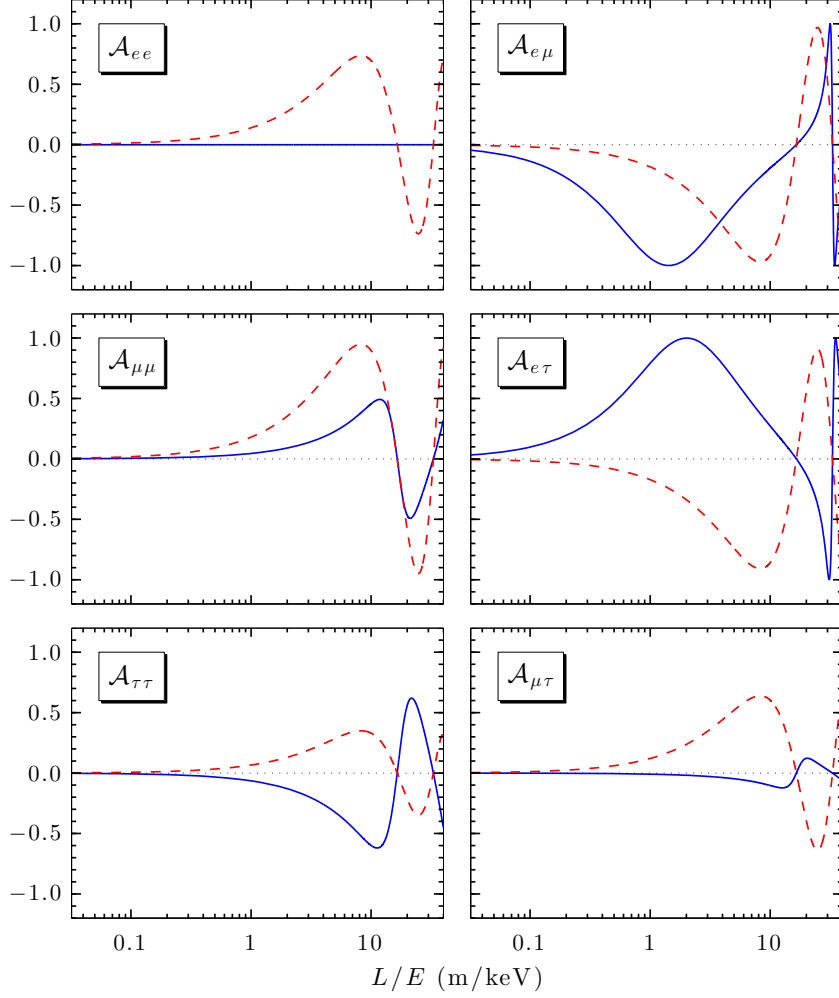


Figure 11: The CP-violating asymmetries $\mathcal{A}_{\alpha\beta}$ versus L/E in the inverted neutrino mass hierarchy with $m_3 = 0$: (a) $\delta = 0^\circ$ and $\rho - \sigma = 45^\circ$ (red dashed lines); (b) $\delta = 90^\circ$ and $\rho - \sigma = 0^\circ$ (blue solid lines).

or take too special values.

When $L/E \gg \mathcal{O}(1)$ m/keV, all the CP-violating asymmetries are averaged out to zero in this special normal mass hierarchy. Hence a measurement of $\mathcal{A}_{\alpha\beta}$ should better be done at $L/E \sim \mathcal{O}(1)$ m/keV. A proper arrangement of L/E may also maximize the signals of CP and T violation.

(B) The inverted neutrino mass hierarchy with $m_3 = 0$. In this case we have $m_2 = \sqrt{-\Delta m_{32}^2} \simeq 4.93 \times 10^{-2}$ eV and $m_1 = \sqrt{-\Delta m_{21}^2 - \Delta m_{32}^2} \simeq 4.85 \times 10^{-2}$ eV. Eq. (12) is then simplified to

$$\mathcal{A}_{\alpha\beta} = \frac{2\mathcal{V}_{\alpha\beta}^{12} \sin 2\phi_{21}}{\sqrt{\frac{\Delta m_{21}^2 + \Delta m_{32}^2}{\Delta m_{32}^2} \mathcal{C}_{\alpha\beta}^{11}} + \sqrt{\frac{\Delta m_{32}^2}{\Delta m_{21}^2 + \Delta m_{32}^2} \mathcal{C}_{\alpha\beta}^{22} + 2\mathcal{C}_{\alpha\beta}^{12} \cos 2\phi_{21}}}. \quad (38)$$

Because of $\Delta m_{21}^2 \ll |\Delta m_{32}^2|$, the coefficients of $\mathcal{C}_{\alpha\beta}^{11}$ and $\mathcal{C}_{\alpha\beta}^{22}$ in Eq. (38) are almost equal to one. So the dependence of $\mathcal{A}_{\alpha\beta}$ on these two mass-squared differences is rather weak. Note that all the $\mathcal{A}_{\alpha\beta}$ do not depend on the absolute values of ρ and σ in the $m_3 = 0$ limit, but they depend on $\rho - \sigma$ and δ . To illustrate, we typically choose $(\delta, \rho - \sigma) = (90^\circ, 0^\circ)$ and $(0^\circ, 45^\circ)$ to calculate the CP-violating asymmetries $\mathcal{A}_{\alpha\beta}$. The numerical results are shown in Figure 11. Some discussions are in order.

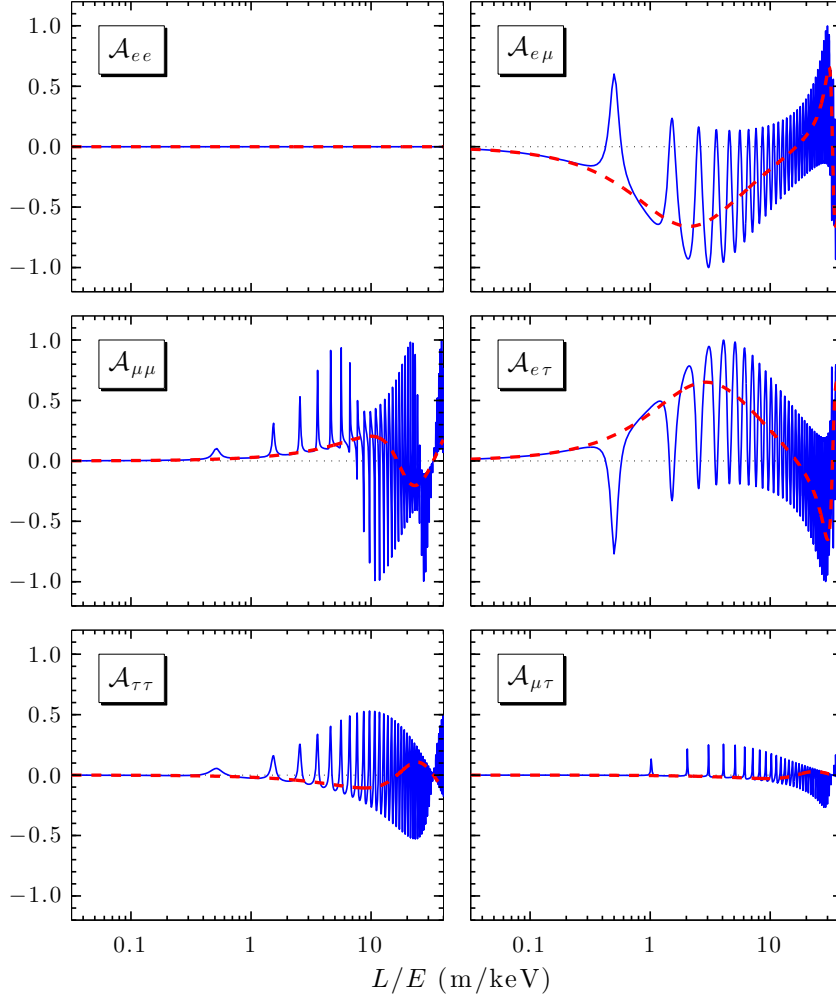


Figure 12: The CP-violating asymmetries $\mathcal{A}_{\alpha\beta}$ (blue solid lines) versus L/E in the nearly degenerate neutrino mass hierarchy with $m_1 \simeq m_2 \simeq m_3$, $\rho = \sigma = 0^\circ$ and $\delta = 90^\circ$, where the red dashed lines stand for $\mathcal{A}_{\alpha\beta}^{21}$ in Eq. (40) with the oscillations driven by Δm_{31}^2 and Δm_{32}^2 being averaged out.

- We see again that switching off the “Dirac” phase δ cannot forbid CP and T violation in neutrino-antineutrino oscillations. Instead, nontrivial values of $\rho - \sigma$ may give rise to significant CP-violating effects in all the channels under discussion.
- Switching off $\rho - \sigma$ can only lead to $\mathcal{A}_{ee} = 0$, simply because $\mathcal{V}_{ee}^{12} = 0$ holds in this case. Thanks to the “Dirac” phase δ , large CP-violating asymmetries between $\nu_\alpha \rightarrow \bar{\nu}_\beta$ and $\bar{\nu}_\alpha \rightarrow \nu_\beta$ oscillations are possible to show up.
- In either case it is possible to achieve the so-called “maximal CP violation” (i.e., $|\mathcal{A}_{\alpha\beta}| = 1$). For example, $|\mathcal{A}_{e\mu}| \simeq 1$ and $|\mathcal{A}_{e\tau}| \simeq 1$ can be obtained for proper values of L/E . Even $|\mathcal{A}_{\mu\mu}|$ may reach its maximal value at a suitable point of L/E [6].

In general, both δ and $\rho - \sigma$ are the sources of CP and T violation. Since δ is always associated with s_{13} , its contribution to $\mathcal{A}_{\alpha\beta}$ is somewhat suppressed as compared with the contribution from $\rho - \sigma$. This point can be clearly seen in Eqs. (19)–(24). Nevertheless, the interplay of δ and $\rho - \sigma$ sometimes plays the dominant role in determining the size of $\mathcal{A}_{\alpha\beta}$.

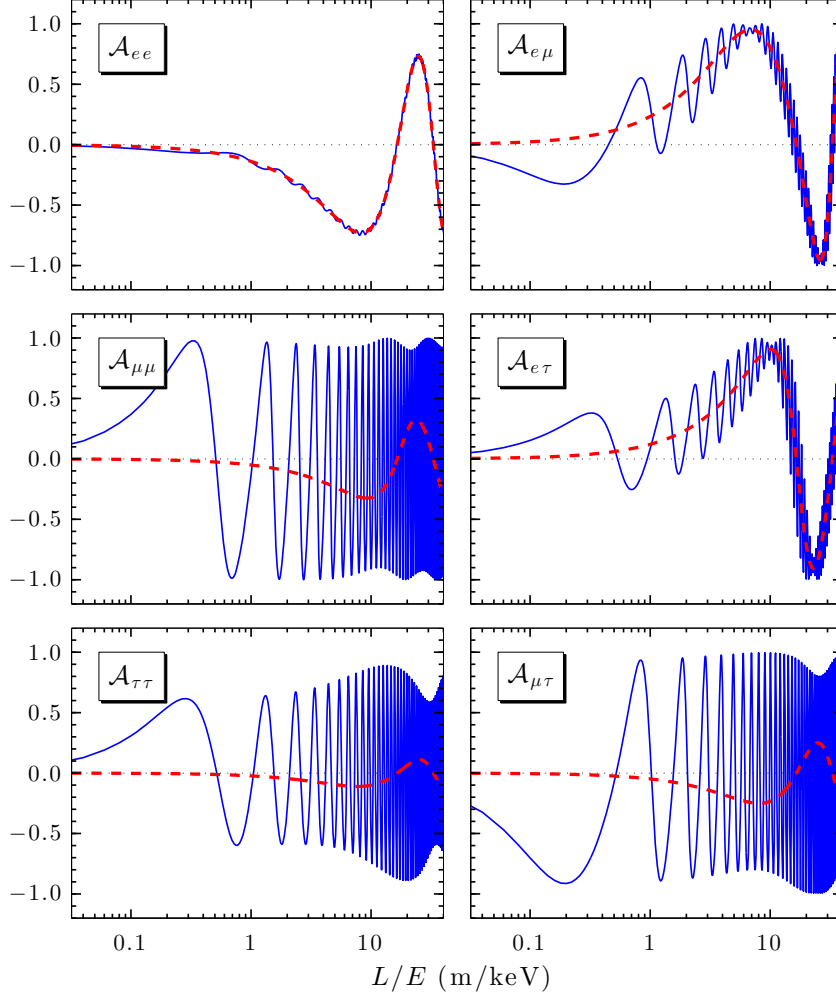


Figure 13: The CP-violating asymmetries $\mathcal{A}_{\alpha\beta}$ (blue solid lines) versus L/E in the nearly degenerate neutrino mass hierarchy with $m_1 \simeq m_2 \simeq m_3$, $\rho = 0^\circ$, $\sigma = 45^\circ$ and $\delta = 90^\circ$, where the red dashed lines stand for $\mathcal{A}_{\alpha\beta}^{21}$ in Eq. (40) with the oscillations driven by Δm_{31}^2 and Δm_{32}^2 being averaged out.

(C) The nearly degenerate mass hierarchy with $m_1 \simeq m_2 \simeq m_3$. In this case $m_i \simeq m_j$ can be factored out and thus canceled on the right-hand side of Eq. (12), leading to the approximate expressions

$$\mathcal{A}_{\alpha\beta} \simeq \frac{2 \sum_{i<j} \mathcal{V}_{\alpha\beta}^{ij} \sin 2\phi_{ji}}{\sum_i \mathcal{C}_{\alpha\beta}^{ii} + 2 \sum_{i<j} \mathcal{C}_{\alpha\beta}^{ij} \cos 2\phi_{ji}}, \quad (39)$$

which are free from the absolute neutrino masses. In view of Eqs. (35) and (36), we approximately have

$$\begin{aligned} \mathcal{A}_{\alpha\beta}^{31} &\simeq \frac{2 (\mathcal{V}_{\alpha\beta}^{13} + \mathcal{V}_{\alpha\beta}^{23}) \sin 2\phi_{31}}{\sum_i \mathcal{C}_{\alpha\beta}^{ii} + 2\mathcal{C}_{\alpha\beta}^{12} + 2 (\mathcal{C}_{\alpha\beta}^{13} + \mathcal{C}_{\alpha\beta}^{23}) \cos 2\phi_{31}}, \\ \mathcal{A}_{\alpha\beta}^{21} &\simeq \frac{2\mathcal{V}_{\alpha\beta}^{12} \sin 2\phi_{21}}{\sum_i \mathcal{C}_{\alpha\beta}^{ii} + 2\mathcal{C}_{\alpha\beta}^{12} \cos 2\phi_{21}}, \end{aligned} \quad (40)$$

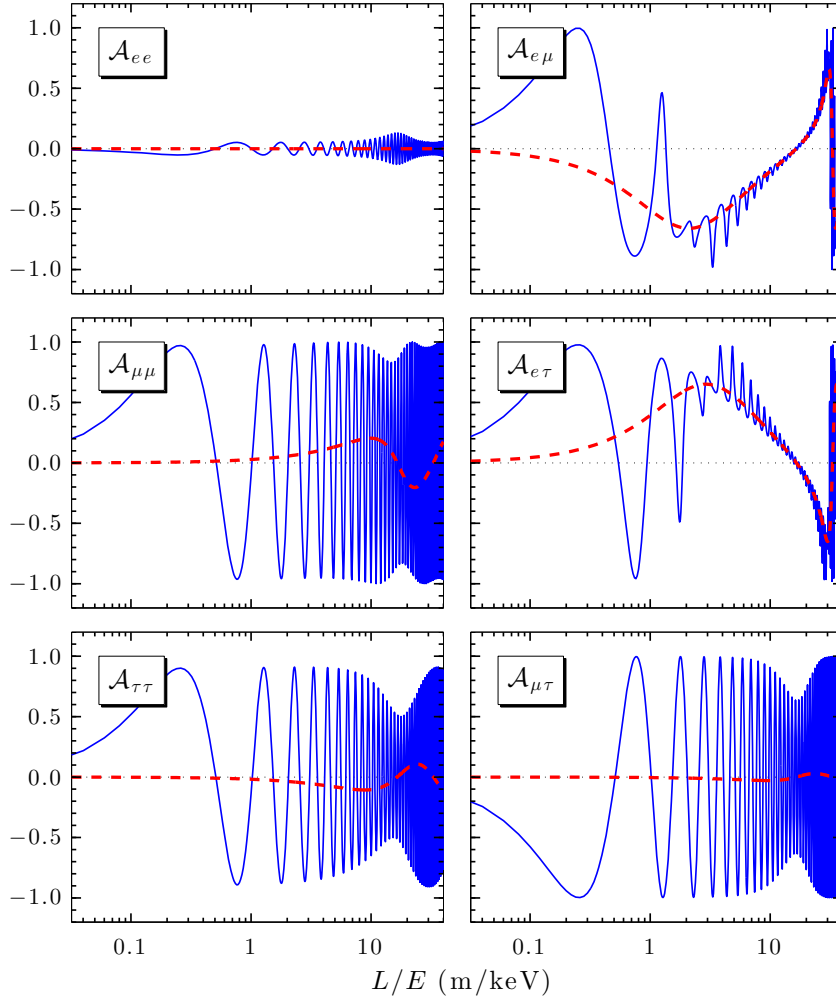


Figure 14: The CP-violating asymmetries $\mathcal{A}_{\alpha\beta}$ (blue solid lines) versus L/E in the nearly degenerate neutrino mass hierarchy with $m_1 \simeq m_2 \simeq m_3$, $\rho = \sigma = 45^\circ$ and $\delta = 90^\circ$, where the red dashed lines stand for $\mathcal{A}_{\alpha\beta}^{21}$ in Eq. (40) with the oscillations driven by Δm_{31}^2 and Δm_{32}^2 being averaged out.

corresponding to the oscillating regions dominated by Δm_{31}^2 (or Δm_{32}^2) and Δm_{21}^2 , respectively. Note that $\mathcal{A}_{\alpha\beta}^{31}$ are sensitive to all the three CP-violating phases, but only the phase difference $\rho - \sigma$ and the “Dirac” phase δ affect $\mathcal{A}_{\alpha\beta}^{21}$. For the purpose of illustration, we typically take $(\rho, \sigma, \delta) = (0^\circ, 0^\circ, 90^\circ)$, $(0^\circ, 45^\circ, 90^\circ)$ and $(45^\circ, 45^\circ, 90^\circ)$ to calculate $\mathcal{A}_{\alpha\beta}$. The numerical results are given in Figures 12–14⁵. Some comments and discussions are in order.

- Figure 12 illustrates the CP-violating effects in neutrino-antineutrino oscillations induced purely by the “Dirac” phase δ . We see that $\mathcal{A}_{ee} = 0$ holds in this case, simply because the input $\delta = 90^\circ$ is too special to generate nonvanishing \mathcal{V}_{ee}^{13} and \mathcal{V}_{ee}^{23} , as shown in Eq. (19). When L/E is sufficiently large, the Δm_{31}^2 - and Δm_{32}^2 -dominated terms oscillate too fast and the observable behaviors of $\mathcal{A}_{\alpha\beta}$ are essentially described by $\mathcal{A}_{\alpha\beta}^{21}$. Once again we conclude that the CP-violating asymmetries $\mathcal{A}_{e\mu}$ and $\mathcal{A}_{e\tau}$ are most sensitive to δ . The same observation is true for the CP-violating asymmetry between normal $\nu_e \rightarrow \nu_\mu$ (or $\nu_e \rightarrow \nu_\tau$) and $\bar{\nu}_e \rightarrow \bar{\nu}_\mu$ (or $\bar{\nu}_e \rightarrow \bar{\nu}_\tau$) oscillations.

⁵We have simply assumed the normal mass hierarchy and input $m_1 = 0.1$ eV in our numerical calculations. We find that the relevant results are almost the same if the inverted mass hierarchy with $m_3 = 0.1$ eV is taken into account.

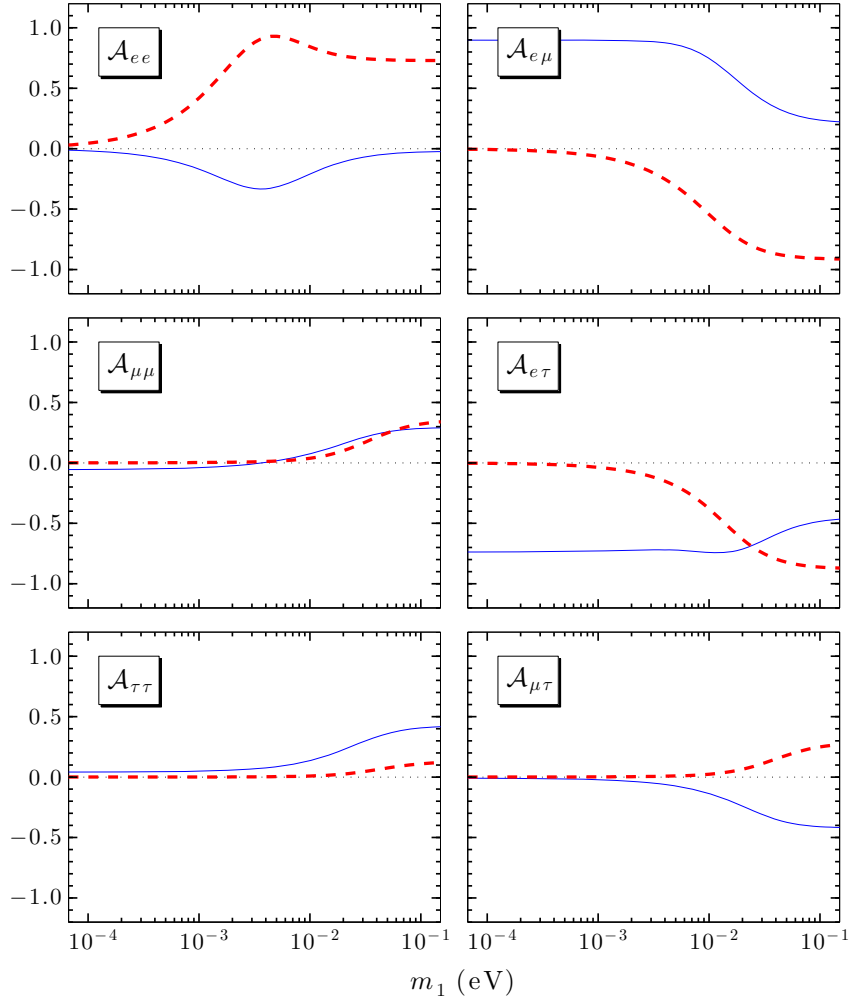


Figure 15: The CP-violating asymmetries $\mathcal{A}_{\alpha\beta}$ versus the lightest neutrino mass m_1 in the normal hierarchy with $\rho = 45^\circ$, $\sigma = 0^\circ$ and $\delta = 90^\circ$, where the blue solid lines and red dashed lines correspond to $L/E \simeq 0.25$ m/keV and 8 m/keV, respectively.

- Figure 13 illustrates the interplay of σ and δ in generating CP and T violation in neutrino-antineutrino oscillations. The suppressed CP-violating asymmetries in Figure 12 (because of $\rho = \sigma = 0^\circ$) are now enhanced to a large extent. When both ρ and σ are switched on, as shown in Figure 14, the situation becomes somewhat more complicated. In either case it is possible to achieve significant or even maximal CP-violating asymmetries. In the oscillating region dominated by Δm_{31}^2 and Δm_{32}^2 , the first maximum or minimum of $\mathcal{A}_{\alpha\beta}$ should be a good place to be detected.
- The first maximum or minimum of $\mathcal{A}_{\alpha\beta}$ in the Δm_{31}^2 -dominated oscillating region roughly occurs around $L/E \sim 0.25$ m/keV, which corresponds to $\phi_{31} \sim \pi/4$. In comparison, the first maximum or minimum of $\mathcal{A}_{\alpha\beta}$ in the Δm_{21}^2 -dominated oscillating region may happen around $L/E \sim 8$ m/keV, corresponding to $\phi_{21} \sim \pi/4$. Of course, these results are more or less subject to the chosen inputs.

The above examples have illustrated the dependence of $\mathcal{A}_{\alpha\beta}$ on the ratio L/E and the three CP-violating phases in three special cases of the neutrino mass spectrum. In the subsequent subsection we shall examine the sensitivity of $\mathcal{A}_{\alpha\beta}$ to the absolute neutrino mass scale in a more careful way.

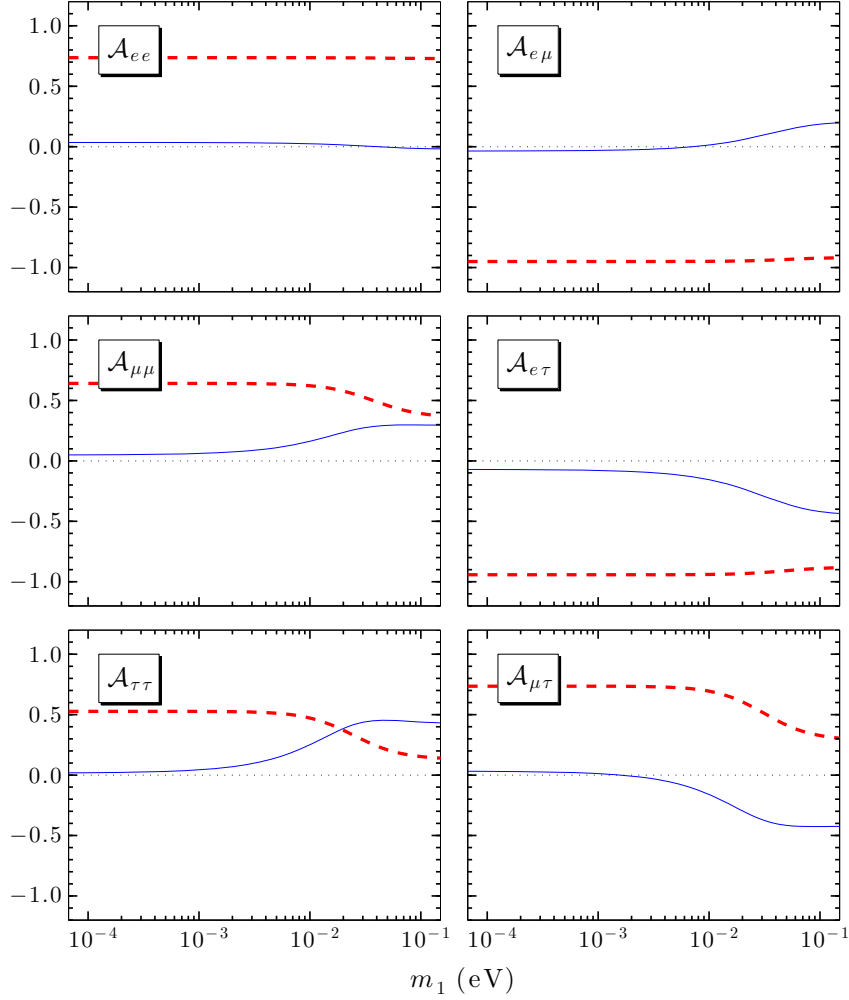


Figure 16: The CP-violating asymmetries $\mathcal{A}_{\alpha\beta}$ versus the lightest neutrino mass m_3 in the inverted hierarchy with $\rho = 45^\circ$, $\sigma = 0^\circ$ and $\delta = 90^\circ$, where the blue solid lines and red dashed lines correspond to $L/E \simeq 0.25$ m/keV and 8 m/keV, respectively.

4.2 The sensitivity of $\mathcal{A}_{\alpha\beta}$ to m_1 or m_3

To simplify our numerical calculations, we typically choose $L/E \simeq 0.25$ m/keV (i.e., $\phi_{31} \simeq \pi/4$) and 8 m/keV (i.e., $\phi_{21} \simeq \pi/4$) which correspond to the Δm_{31}^2 - and Δm_{21}^2 -dominated oscillating regions, respectively. We also fix $\rho = 45^\circ$, $\sigma = 0^\circ$ and $\delta = 90^\circ$ to see the changes of $\mathcal{A}_{\alpha\beta}$ with the lightest neutrino mass m_1 (normal hierarchy) or m_3 (inverted hierarchy). The numerical results are shown in Figures 15 and 16. Some comments are in order.

- In Figure 15 the values of m_1 change from $\mathcal{O}(10^{-4})$ eV to $\mathcal{O}(10^{-1})$ eV, implying the changes of the neutrino mass spectrum from $m_1 \ll m_2 \ll m_3$ to $m_1 \lesssim m_2 \lesssim m_3$. The turning point is roughly $m_1 \sim \sqrt{\Delta m_{31}^2}$, around which the sensitivity of $\mathcal{A}_{\alpha\beta}$ to m_1 becomes stronger. In the chosen parameter space we find that \mathcal{A}_{ee} , $\mathcal{A}_{e\mu}$ and $\mathcal{A}_{e\tau}$ are most sensitive to m_1 at $L/E \simeq 8$ m/keV: the results of these three CP-violating asymmetries for $m_1 \simeq 0.1$ eV are significantly different from the ones for $m_1 \simeq 0$.
- In Figure 16 the values of m_3 change from $\mathcal{O}(10^{-4})$ eV to $\mathcal{O}(10^{-1})$ eV, implying the changes of the

neutrino mass spectrum from $m_3 \ll m_1 \lesssim m_2$ to $m_3 \lesssim m_1 \lesssim m_2$. The turning point is roughly $m_3 \sim \sqrt{|\Delta m_{32}^2|}$, around which the sensitivity of $\mathcal{A}_{\alpha\beta}$ to m_3 becomes more appreciable. But a comparison between Figures 15 and 16 tells us that the CP-violating asymmetries are in general less sensitive to the absolute neutrino mass scale in the case of the inverted hierarchy.

- As for the results of $\mathcal{A}_{\alpha\beta}$, it does not make much difference whether the nearly degenerate neutrino mass spectrum is $m_1 \lesssim m_2 \lesssim m_3$ or $m_3 \lesssim m_1 \lesssim m_2$. This point can be clearly seen in Figures 15 and 16 at $m_1 \simeq m_3 \simeq 0.1$ eV, where the numerical results in these two nearly degenerate mass spectra approximately match each other.

So it is in principle possible to probe the absolute neutrino mass scale through the study of neutrino-antineutrino oscillation. In comparison, the normal neutrino-neutrino and antineutrino-antineutrino oscillations are only sensitive to the neutrino mass-squared differences.

5 Summary

One of the fundamental questions about massive neutrinos is what their nature is or whether they are the Dirac or Majorana particles. The absolute neutrino mass scale is so low that it is extremely difficult to distinguish between the Dirac and Majorana neutrinos in all the currently available experiments. Today's techniques have allowed us to push the sensitivity of the $0\nu\beta\beta$ decay to the level of $|\langle m \rangle_{ee}| \sim \mathcal{O}(0.1)$ eV, making it the most feasible way to probe the Majorana nature of massive neutrinos. The present work is just motivated by a meaningful question that we have asked ourselves: what can we proceed to do to determine all the CP-violating phases in the PMNS matrix U if the massive neutrinos are someday identified *to be* the Majorana particles through a convincing measurement of the $0\nu\beta\beta$ decay?

In principle, one may determine the Majorana phases of U in neutrino-antineutrino oscillations ⁶. In practice, such an experiment might only be feasible in the very distant future. But we find that a systematic study of CP violation in neutrino-antineutrino oscillations is still useful, so as to enrich the phenomenology of Majorana neutrinos. In this work we have explored the salient features of three-flavor neutrino-antineutrino oscillations and their CP- and T-violating asymmetries. Six independent $0\nu\beta\beta$ -like mass terms $\langle m \rangle_{\alpha\beta}$ and nine independent Jalskog-like parameters $\mathcal{V}_{\alpha\beta}^{ij}$ have been analyzed in detail, because they are quite universal and can contribute to the CP-conserving and CP-violating parts of a number of LNV processes. We have made a comparison between $\mathcal{V}_{\alpha\beta}^{ij}$ and the Jarlskog invariant \mathcal{J} by switching off the Majorana phases ρ and σ , and have demonstrated the Majorana nature of the ‘‘Dirac’’ phase δ . As a by-product, the effects of three CP-violating phases on the LNV decays of doubly- and singly-charged Higgs bosons have also been reexamined. We have carried out a comprehensive analysis of the sensitivities of six possible CP-violating asymmetries $\mathcal{A}_{\alpha\beta}$ to the three phase parameters, the neutrino mass spectrum and the ratio of the neutrino beam energy E to the baseline length L . Our analytical and numerical results provide a complete description of the distinct roles of Majorana CP-violating phases in neutrino-antineutrino oscillations and other LNV processes.

Although the particular parametrization of U advocated by the Particle Data Group [4] has been used in this work, one may always choose a different representation of U which might be more convenient

⁶Because the Dirac neutrinos do not violate the lepton number, they cannot undergo neutrino-antineutrino oscillations. However, it is likely for the Dirac neutrinos to oscillate between their left-handed and right-handed states in a magnetic field and in the presence of matter effects [25]. Such spin-flavor precession processes are beyond the scope of the present paper and will be further studied elsewhere.

in some aspects of the Majorana neutrino phenomenology. For instance, the so-called ‘‘symmetrical parametrization’’ of the PMNS matrix [26]

$$K = \begin{pmatrix} c_{12}c_{13} & s_{12}c_{13}e^{-i\varphi_{12}} & s_{13}e^{-i\varphi_{13}} \\ -s_{12}c_{23}e^{i\varphi_{12}} - c_{12}s_{13}s_{23}e^{-i(\varphi_{23}-\varphi_{13})} & c_{12}c_{23} - s_{12}s_{13}s_{23}e^{-i(\varphi_{12}+\varphi_{23}-\varphi_{13})} & c_{13}s_{23}e^{-i\varphi_{23}} \\ s_{12}s_{23}e^{i(\varphi_{12}+\varphi_{23})} - c_{12}s_{13}c_{23}e^{i\varphi_{13}} & -c_{12}s_{23}e^{i\varphi_{23}} - s_{12}s_{13}c_{23}e^{-i(\varphi_{12}-\varphi_{13})} & c_{13}c_{23} \end{pmatrix} \quad (41)$$

has also been used by some authors to describe neutrino oscillations and LNV processes [27]. It is easy to establish the relationship between U in Eq. (1) and K in Eq. (41):

$$U = \begin{pmatrix} e^{i\rho} & 0 & 0 \\ 0 & e^{i\sigma} & 0 \\ 0 & 0 & 1 \end{pmatrix} K, \quad (42)$$

where the three phase parameters of U are related to the three phase parameters of K as follows:

$$\begin{aligned} \delta &= \varphi_{13} - \varphi_{12} - \varphi_{23}, \\ \rho &= \varphi_{12} + \varphi_{23}, \\ \sigma &= \varphi_{23}. \end{aligned} \quad (43)$$

Therefore, it is straightforward to reexpress $\mathcal{C}_{\alpha\beta}^{ij}$ and $\mathcal{V}_{\alpha\beta}^{ij}$ in terms of the angle and phase parameters of K simply with the help of Eq. (43). Given three light or heavy *sterile* neutrinos, it is also straightforward to extend Eq. (41) to a full parametrization of the 6×6 neutrino mixing matrix [28].

The Schechter-Valle (Black Box) theorem [29] has told us that an observation of the $0\nu\beta\beta$ decay points to the Majorana nature of massive neutrinos, but such a LNV process may be dominated either by a tree-level Majorana neutrino mass term or by other possible new physics which is essentially unrelated to the neutrino masses. The radiative mass term induced by the Black Box (loop) diagram itself is extremely small in most cases, although this is not always true [30]. Hence one has to be careful when relating the rate of the $0\nu\beta\beta$ decay fully to the neutrino masses. In this work we have assumed the existence of a tree-level Majorana mass term dominating the Black Box diagram, leading to $\langle m \rangle_{ee}$ which has a direct relation to the rate of the $0\nu\beta\beta$ decay. The same observation is expected to be true for all the LNV processes which depend on the effective Majorana mass terms $\langle m \rangle_{\alpha\beta}$. Of course, the situation will change if other types of LNV physics exist [30].

While it is still a dream to fully determine the flavor dynamics of Majorana neutrinos, including their CP-violating phases, one should not be too pessimistic. The reason is simply that the history of neutrino physics has been full of surprises in making the impossible possible, but one has to be patient.

Acknowledgement

We would like to thank Y.F. Li for helpful discussions. This work was supported in part by the National Natural Science Foundation of China under Grant No. 11135009.

A Explicit expressions of $\mathcal{C}_{\alpha\beta}^{ij}$

Given the standard parametrization of the PMNS matrix U in Eq. (1), one may explicitly write out all the CP-conserving quantities $\mathcal{C}_{\alpha\beta}^{ij}$ defined in Eq. (5). Such formulas are expected to be useful to understand the behaviors of neutrino-antineutrino oscillations and make reasonable analytical approximations for their oscillation probabilities and CP-violating asymmetries.

First of all, we have $\mathcal{C}_{\alpha\alpha}^{ii} = |U_{\alpha i}|^4$ (for $\alpha = e, \mu, \tau$ and $i = 1, 2, 3$). The explicit expressions of these nine quantities are

$$\begin{aligned}
\mathcal{C}_{ee}^{11} &= c_{12}^4 c_{13}^4, \\
\mathcal{C}_{ee}^{22} &= s_{12}^4 c_{13}^4, \\
\mathcal{C}_{ee}^{33} &= s_{13}^4; \\
\mathcal{C}_{\mu\mu}^{11} &= (s_{12}^2 c_{23}^2 + 2c_{12}s_{12}s_{13}c_{23}s_{23}\cos\delta + c_{12}^2 s_{13}^2 s_{23}^2)^2, \\
\mathcal{C}_{\mu\mu}^{22} &= (c_{12}^2 c_{23}^2 - 2c_{12}s_{12}s_{13}c_{23}s_{23}\cos\delta + s_{12}^2 s_{13}^2 s_{23}^2)^2, \\
\mathcal{C}_{\mu\mu}^{33} &= c_{13}^4 s_{23}^4; \\
\mathcal{C}_{\tau\tau}^{11} &= (s_{12}^2 s_{23}^2 - 2c_{12}s_{12}s_{13}c_{23}s_{23}\cos\delta + c_{12}^2 s_{13}^2 c_{23}^2)^2, \\
\mathcal{C}_{\tau\tau}^{22} &= (c_{12}^2 s_{23}^2 + 2c_{12}s_{12}s_{13}c_{23}s_{23}\cos\delta + s_{12}^2 s_{13}^2 c_{23}^2)^2, \\
\mathcal{C}_{\tau\tau}^{33} &= c_{13}^4 c_{23}^4.
\end{aligned} \tag{44}$$

Because $\mathcal{C}_{\alpha\beta}^{ii} = \sqrt{\mathcal{C}_{\alpha\alpha}^{ii}\mathcal{C}_{\beta\beta}^{ii}}$ holds, it is straightforward to write out the expressions of $\mathcal{C}_{\alpha\beta}^{ii}$ (for $\alpha \neq \beta$) with the help of Eq. (44). The following sum rule is also valid:

$$\sum_{\alpha} \sum_{\beta} \mathcal{C}_{\alpha\beta}^{ii} = \sum_{\alpha} |U_{\alpha i}|^2 = 1. \tag{45}$$

We see that all the $\mathcal{C}_{\alpha\beta}^{ii}$ are independent of the Majorana phases ρ and σ .

Next, we calculate $\mathcal{C}_{\alpha\alpha}^{ij}$ and $\mathcal{C}_{\alpha\beta}^{ij}$ in terms of the flavor mixing parameters of the PMNS matrix U given in Eq. (1). The results are

$$\begin{aligned}
\mathcal{C}_{ee}^{12} &= c_{12}^2 s_{12}^2 c_{13}^4 \cos 2(\rho - \sigma), \\
\mathcal{C}_{ee}^{13} &= c_{12}^2 c_{13}^2 s_{13}^2 \cos 2(\delta + \rho), \\
\mathcal{C}_{ee}^{23} &= s_{12}^2 c_{13}^2 s_{13}^2 \cos 2(\delta + \sigma); \\
\mathcal{C}_{\mu\mu}^{12} &= c_{12}^2 s_{12}^2 (c_{23}^4 - 4s_{13}^2 c_{23}^2 s_{23}^2 + s_{13}^4 s_{23}^4) \cos 2(\rho - \sigma) \\
&\quad + 2c_{12}s_{12}s_{13}c_{23}s_{23} (c_{23}^2 - s_{13}^2 s_{23}^2) [c_{12}^2 \cos(2\rho - 2\sigma + \delta) - s_{12}^2 \cos(2\rho - 2\sigma - \delta)] \\
&\quad + s_{13}^2 c_{23}^2 s_{23}^2 [c_{12}^4 \cos 2(\rho - \sigma + \delta) + s_{12}^4 \cos 2(\rho - \sigma - \delta)], \\
\mathcal{C}_{\mu\mu}^{13} &= c_{13}^2 s_{23}^2 [s_{12}^2 c_{23}^2 \cos 2\rho + 2c_{12}s_{12}s_{13}c_{23}s_{23} \cos(\delta + 2\rho) + c_{12}^2 s_{13}^2 s_{23}^2 \cos 2(\delta + \rho)], \\
\mathcal{C}_{\mu\mu}^{23} &= c_{13}^2 s_{23}^2 [c_{12}^2 c_{23}^2 \cos 2\sigma - 2c_{12}s_{12}s_{13}c_{23}s_{23} \cos(\delta + 2\sigma) + s_{12}^2 s_{13}^2 s_{23}^2 \cos 2(\delta + \sigma)]; \\
\mathcal{C}_{\tau\tau}^{12} &= c_{12}^2 s_{12}^2 (s_{23}^4 - 4s_{13}^2 c_{23}^2 s_{23}^2 + s_{13}^4 c_{23}^4) \cos 2(\rho - \sigma) \\
&\quad - 2c_{12}s_{12}s_{13}c_{23}s_{23} (s_{23}^2 - s_{13}^2 c_{23}^2) [c_{12}^2 \cos(2\rho - 2\sigma + \delta) - s_{12}^2 \cos(2\rho - 2\sigma - \delta)] \\
&\quad + s_{13}^2 c_{23}^2 s_{23}^2 [c_{12}^4 \cos 2(\rho - \sigma + \delta) + s_{12}^4 \cos 2(\rho - \sigma - \delta)], \\
\mathcal{C}_{\tau\tau}^{13} &= c_{13}^2 c_{23}^2 [s_{12}^2 s_{23}^2 \cos 2\rho - 2c_{12}s_{12}s_{13}c_{23}s_{23} \cos(\delta + 2\rho) + c_{12}^2 s_{13}^2 c_{23}^2 \cos 2(\delta + \rho)], \\
\mathcal{C}_{\tau\tau}^{23} &= c_{13}^2 c_{23}^2 [c_{12}^2 s_{23}^2 \cos 2\sigma + 2c_{12}s_{12}s_{13}c_{23}s_{23} \cos(\delta + 2\sigma) + s_{12}^2 s_{13}^2 c_{23}^2 \cos 2(\delta + \sigma)];
\end{aligned} \tag{46}$$

and

$$\begin{aligned}
\mathcal{C}_{e\mu}^{12} &= -c_{12}^2 s_{12}^2 c_{13}^2 (c_{23}^2 - s_{13}^2 s_{23}^2) \cos 2(\rho - \sigma) \\
&\quad - c_{12} s_{12} c_{13}^2 s_{13} c_{23} s_{23} [c_{12}^2 \cos(2\rho - 2\sigma + \delta) - s_{12}^2 \cos(2\rho - 2\sigma - \delta)] , \\
\mathcal{C}_{e\mu}^{13} &= -c_{12} c_{13}^2 s_{13} s_{23} [s_{12} c_{23} \cos(\delta + 2\rho) - c_{12} s_{13} s_{23} \cos 2(\delta + \rho)] , \\
\mathcal{C}_{e\mu}^{23} &= +s_{12} c_{13}^2 s_{13} s_{23} [c_{12} c_{23} \cos(\delta + 2\sigma) - s_{12} s_{13} s_{23} \cos 2(\delta + \sigma)] ; \\
\mathcal{C}_{e\tau}^{12} &= c_{12}^2 s_{12}^2 c_{13}^2 (c_{23}^2 s_{13}^2 - s_{23}^2) \cos 2(\rho - \sigma) \\
&\quad + c_{12} s_{12} c_{13}^2 s_{13} c_{23} s_{23} [c_{12}^2 \cos(2\rho - 2\sigma + \delta) - s_{12}^2 \cos(2\rho - 2\sigma - \delta)] , \\
\mathcal{C}_{e\tau}^{13} &= +c_{12} c_{13}^2 s_{13} c_{23} [s_{12} s_{23} \cos(\delta + 2\rho) - c_{12} s_{13} c_{23} \cos 2(\delta + \rho)] , \\
\mathcal{C}_{e\tau}^{23} &= -s_{12} c_{13}^2 s_{13} c_{23} [c_{12} s_{23} \cos(\delta + 2\sigma) + s_{12} s_{13} c_{23} \cos 2(\delta + \sigma)] ; \\
\mathcal{C}_{\mu\tau}^{12} &= -c_{12}^2 s_{12}^2 [c_{23}^4 s_{13}^2 - (1 + s_{13}^2)^2 c_{23}^2 s_{23}^2 + s_{13}^2 s_{23}^4] \cos 2(\rho - \sigma) \\
&\quad - c_{12} s_{12} s_{13} c_{23} s_{23} (1 + s_{13}^2) (c_{23}^2 - s_{23}^2) [c_{12}^2 \cos(2\rho - 2\sigma + \delta) - s_{12}^2 \cos(2\rho - 2\sigma - \delta)] \\
&\quad - s_{13}^2 c_{23}^2 s_{23}^2 [c_{12}^4 \cos 2(\rho - \sigma + \delta) + s_{12}^4 \cos 2(\rho - \sigma - \delta)] , \\
\mathcal{C}_{\mu\tau}^{13} &= c_{13}^2 c_{23} s_{23} [-s_{12}^2 c_{23} s_{23} \cos 2\rho + c_{12} s_{12} s_{13} (c_{23}^2 - s_{23}^2) \cos(\delta + 2\rho) + c_{12}^2 s_{13}^2 c_{23} s_{23} \cos 2(\delta + \rho)] , \\
\mathcal{C}_{\mu\tau}^{23} &= c_{13}^2 c_{23} s_{23} [-c_{12}^2 c_{23} s_{23} \cos 2\sigma - c_{12} s_{12} s_{13} (c_{23}^2 - s_{23}^2) \cos(\delta + 2\sigma) + s_{12}^2 s_{13}^2 c_{23} s_{23} \cos 2(\delta + \sigma)] . \quad (47)
\end{aligned}$$

By definition, $\mathcal{C}_{\alpha\beta}^{ij} = \mathcal{C}_{\beta\alpha}^{ji} = \mathcal{C}_{\alpha\beta}^{ji} = \mathcal{C}_{\beta\alpha}^{ij}$ holds. Then Eq. (8) allows us to establish the following relations between the results of $\mathcal{C}_{\alpha\alpha}^{ij}$ in Eq. (46) and those of $\mathcal{C}_{\alpha\beta}^{ij}$ in Eq. (47):

$$\begin{aligned}
\mathcal{C}_{e\mu}^{ij} &= \frac{1}{2} (\mathcal{C}_{\tau\tau}^{ij} - \mathcal{C}_{ee}^{ij} - \mathcal{C}_{\mu\mu}^{ij}) , \\
\mathcal{C}_{\mu\tau}^{ij} &= \frac{1}{2} (\mathcal{C}_{ee}^{ij} - \mathcal{C}_{\mu\mu}^{ij} - \mathcal{C}_{\tau\tau}^{ij}) , \\
\mathcal{C}_{\tau e}^{ij} &= \frac{1}{2} (\mathcal{C}_{\mu\mu}^{ij} - \mathcal{C}_{ee}^{ij} - \mathcal{C}_{\tau\tau}^{ij}) . \quad (48)
\end{aligned}$$

In view of the smallness of θ_{13} , one may make some analytical approximations for the above results by neglecting the terms proportional to s_{13}^2 .

B Analytical approximations of $\langle m \rangle_{\alpha\beta}$

The exact expressions of $\langle m \rangle_{\alpha\beta}$ have been given in Eq. (27). To understand Figure 4 in a better way, here we make some analytical approximations for all the $|\langle m \rangle_{\alpha\beta}|$ in four special but interesting cases.

Case (A): the lightest neutrino mass m_1 satisfies $m_1^2 \ll \Delta m_{21}^2$. In this case, $m_2 \simeq \sqrt{\Delta m_{21}^2}$ and $m_3 \simeq \sqrt{\Delta m_{31}^2}$ hold. One may therefore neglect those terms proportional to m_1 in Eq. (27). In view of the smallness of θ_{13} , we approximately have

$$\begin{aligned}
\langle m \rangle_{ee} &\simeq +\sqrt{\Delta m_{21}^2} s_{12}^2 e^{2i\sigma} + \sqrt{\Delta m_{31}^2} s_{13}^2 e^{-2i\delta} , \\
\langle m \rangle_{\mu\mu} &\simeq +\sqrt{\Delta m_{21}^2} c_{12}^2 c_{23}^2 e^{2i\sigma} + \sqrt{\Delta m_{31}^2} s_{23}^2 , \\
\langle m \rangle_{\tau\tau} &\simeq +\sqrt{\Delta m_{21}^2} c_{12}^2 s_{23}^2 e^{2i\sigma} + \sqrt{\Delta m_{31}^2} c_{23}^2 , \\
\langle m \rangle_{e\mu} &\simeq +\sqrt{\Delta m_{21}^2} c_{12} s_{12} c_{23} e^{2i\sigma} + \sqrt{\Delta m_{31}^2} s_{13} s_{23} e^{-i\delta} , \\
\langle m \rangle_{e\tau} &\simeq -\sqrt{\Delta m_{21}^2} c_{12} s_{12} s_{23} e^{2i\sigma} + \sqrt{\Delta m_{31}^2} s_{13} c_{23} e^{-i\delta} , \\
\langle m \rangle_{\mu\tau} &\simeq -\sqrt{\Delta m_{21}^2} c_{12}^2 c_{23} s_{23} e^{2i\sigma} + \sqrt{\Delta m_{31}^2} c_{23} s_{23} . \quad (49)
\end{aligned}$$

The lower and upper bounds of $|\langle m \rangle|_{\alpha\beta}$ turn out to be

$$\begin{aligned}
\sqrt{\Delta m_{21}^2} s_{12}^2 - \sqrt{\Delta m_{31}^2} s_{13}^2 &\lesssim |\langle m \rangle_{ee}| \lesssim \sqrt{\Delta m_{21}^2} s_{12}^2 + \sqrt{\Delta m_{31}^2} s_{13}^2, \\
\sqrt{\Delta m_{31}^2} s_{23}^2 - \sqrt{\Delta m_{21}^2} c_{12}^2 c_{23}^2 &\lesssim |\langle m \rangle_{\mu\mu}| \lesssim \sqrt{\Delta m_{31}^2} s_{23}^2 + \sqrt{\Delta m_{21}^2} c_{12}^2 c_{23}^2, \\
\sqrt{\Delta m_{31}^2} c_{23}^2 - \sqrt{\Delta m_{21}^2} c_{12}^2 s_{23}^2 &\lesssim |\langle m \rangle_{\tau\tau}| \lesssim \sqrt{\Delta m_{31}^2} c_{23}^2 + \sqrt{\Delta m_{21}^2} c_{12}^2 s_{23}^2, \\
\sqrt{\Delta m_{31}^2} s_{13} s_{23} - \sqrt{\Delta m_{21}^2} c_{12} s_{12} c_{23} &\lesssim |\langle m \rangle_{e\mu}| \lesssim \sqrt{\Delta m_{31}^2} s_{13} s_{23} + \sqrt{\Delta m_{21}^2} c_{12} s_{12} c_{23}, \\
\sqrt{\Delta m_{31}^2} s_{13} c_{23} - \sqrt{\Delta m_{21}^2} c_{12} s_{12} s_{23} &\lesssim |\langle m \rangle_{e\tau}| \lesssim \sqrt{\Delta m_{31}^2} s_{13} c_{23} + \sqrt{\Delta m_{21}^2} c_{12} s_{12} s_{23}, \\
\sqrt{\Delta m_{31}^2} c_{23} s_{23} - \sqrt{\Delta m_{21}^2} c_{12}^2 c_{23} s_{23} &\lesssim |\langle m \rangle_{\mu\tau}| \lesssim \sqrt{\Delta m_{31}^2} c_{23} s_{23} + \sqrt{\Delta m_{21}^2} c_{12}^2 c_{23} s_{23}. \quad (50)
\end{aligned}$$

We see that the dominant terms of $|\langle m \rangle_{\mu\mu}|$, $|\langle m \rangle_{\tau\tau}|$ and $|\langle m \rangle_{\mu\tau}|$ are associated with $\sqrt{\Delta m_{31}^2}$, and they receive some small corrections from the terms proportional to $\sqrt{\Delta m_{21}^2}$. In comparison, the magnitude of $|\langle m \rangle_{ee}|$ is much smaller because its $\sqrt{\Delta m_{31}^2}$ term is suppressed by s_{13}^2 . The dominant terms of $|\langle m \rangle_{e\mu}|$ and $|\langle m \rangle_{e\tau}|$ are associated with $\sqrt{\Delta m_{31}^2} s_{13}$, and thus they are somewhat less suppressed.

Case (B): the lightest neutrino mass m_3 satisfies $m_3^2 \ll \Delta m_{21}^2$. In this case, $m_1 \simeq m_2 \simeq \sqrt{-\Delta m_{32}^2}$ holds. We are allowed to neglect those terms proportional to m_3 in Eq. (27). Given the smallness of θ_{13} , we approximately obtain

$$\begin{aligned}
\langle m \rangle_{ee} &\simeq +\sqrt{-\Delta m_{32}^2} (c_{12}^2 e^{2i\rho} + s_{12}^2 e^{2i\sigma}), \\
\langle m \rangle_{\mu\mu} &\simeq +\sqrt{-\Delta m_{32}^2} c_{23}^2 (s_{12}^2 e^{2i\rho} + c_{12}^2 e^{2i\sigma}), \\
\langle m \rangle_{\tau\tau} &\simeq +\sqrt{-\Delta m_{32}^2} s_{23}^2 (c_{12}^2 e^{2i\sigma} - s_{12}^2 e^{2i\rho}), \\
\langle m \rangle_{e\mu} &\simeq +\sqrt{-\Delta m_{32}^2} c_{12} s_{12} c_{23} (e^{2i\sigma} - e^{2i\rho}), \\
\langle m \rangle_{e\tau} &\simeq +\sqrt{-\Delta m_{32}^2} c_{12} s_{12} s_{23} (e^{2i\rho} - e^{2i\sigma}), \\
\langle m \rangle_{\mu\tau} &\simeq -\sqrt{-\Delta m_{32}^2} c_{23} s_{23} (s_{12}^2 e^{2i\rho} + c_{12}^2 e^{2i\sigma}). \quad (51)
\end{aligned}$$

Then the lower and upper bounds of $|\langle m \rangle_{\alpha\beta}|$ are approximately given by

$$\begin{aligned}
\sqrt{-\Delta m_{32}^2} \cos 2\theta_{12} &\lesssim |\langle m \rangle_{ee}| \lesssim \sqrt{-\Delta m_{32}^2}, \\
\sqrt{-\Delta m_{32}^2} c_{23}^2 \cos 2\theta_{12} &\lesssim |\langle m \rangle_{\mu\mu}| \lesssim \sqrt{-\Delta m_{32}^2} c_{23}^2, \\
\sqrt{-\Delta m_{32}^2} s_{23}^2 \cos 2\theta_{12} &\lesssim |\langle m \rangle_{\tau\tau}| \lesssim \sqrt{-\Delta m_{32}^2} s_{23}^2, \\
0 &\lesssim |\langle m \rangle_{e\mu}| \lesssim \sqrt{-\Delta m_{32}^2} \sin 2\theta_{12} c_{23}, \\
0 &\lesssim |\langle m \rangle_{e\tau}| \lesssim \sqrt{-\Delta m_{32}^2} \sin 2\theta_{12} s_{23}, \\
\sqrt{-\Delta m_{32}^2} c_{23} s_{23} \cos 2\theta_{12} &\lesssim |\langle m \rangle_{\mu\tau}| \lesssim \sqrt{-\Delta m_{32}^2} c_{23} s_{23}. \quad (52)
\end{aligned}$$

We see that the lower bounds of $|\langle m \rangle_{e\mu}|$ and $|\langle m \rangle_{e\tau}|$ are zero, while the allowed ranges of the other four effective mass terms are quite narrow and at the level of $\sqrt{-\Delta m_{32}^2}$. Given $\rho \simeq \sigma$, even the texture zeros $\langle m \rangle_{e\mu} \simeq \langle m \rangle_{e\tau} \simeq 0$ can be achieved. A systematic analysis of such two-zero textures of the Majorana neutrino mass matrix M_ν has been done in the literature [31].

Case (C): the lightest neutrino mass m_1 satisfies $m_1^2 \gg \Delta m_{31}^2$. This case corresponds to a nearly degenerate mass hierarchy: $m_1 \simeq m_2$ and $m_3 \simeq m_1 + \Delta m_{31}^2/(2m_1)$. Given the smallness of θ_{13} , the expressions of $\langle m \rangle_{\alpha\beta}$ in Eq. (27) approximate to

$$\begin{aligned}
\langle m \rangle_{ee} &\simeq m_1 (c_{12}^2 e^{2i\rho} + s_{12}^2 e^{2i\sigma}) , \\
\langle m \rangle_{\mu\mu} &\simeq m_1 (s_{23}^2 + s_{12}^2 c_{23}^2 e^{2i\rho} + c_{12}^2 c_{23}^2 e^{2i\sigma}) + \frac{\Delta m_{31}^2}{2m_1} s_{23}^2 , \\
\langle m \rangle_{\tau\tau} &\simeq m_1 (c_{23}^2 + c_{12}^2 s_{23}^2 e^{2i\sigma} + s_{12}^2 s_{23}^2 e^{2i\rho}) + \frac{\Delta m_{31}^2}{2m_1} c_{23}^2 , \\
\langle m \rangle_{e\mu} &\simeq m_1 c_{12} s_{12} c_{23} (e^{2i\sigma} - e^{2i\rho}) , \\
\langle m \rangle_{e\tau} &\simeq m_1 c_{12} s_{12} s_{23} (e^{2i\rho} - e^{2i\sigma}) , \\
\langle m \rangle_{\mu\tau} &\simeq m_1 c_{23} s_{23} (1 - c_{12}^2 e^{2i\sigma} - s_{12}^2 e^{2i\rho}) + \frac{\Delta m_{31}^2}{2m_1} c_{23} s_{23} .
\end{aligned} \tag{53}$$

The lower and upper bounds of $|\langle m \rangle_{\alpha\beta}|$ turn out to be

$$\begin{aligned}
m_1 \cos 2\theta_{12} &\lesssim |\langle m \rangle_{ee}| \lesssim m_1 , \\
0 &\lesssim |\langle m \rangle_{\mu\mu}| \lesssim m_1 , \\
m_1 \cos 2\theta_{23} + \frac{\Delta m_{31}^2}{2m_1} c_{23}^2 &\lesssim |\langle m \rangle_{\tau\tau}| \lesssim m_1 , \\
0 &\lesssim |\langle m \rangle_{e\mu}| \lesssim m_1 \sin 2\theta_{12} c_{23} , \\
0 &\lesssim |\langle m \rangle_{e\tau}| \lesssim m_1 \sin 2\theta_{12} s_{23} , \\
\frac{\Delta m_{31}^2}{4m_1} \sin 2\theta_{23} &\lesssim |\langle m \rangle_{\mu\tau}| \lesssim m_1 \sin 2\theta_{23} .
\end{aligned} \tag{54}$$

Note that the lower bounds of $|\langle m \rangle_{\mu\mu}|$ and $|\langle m \rangle_{\tau\tau}|$ obtained above hold only in the $\theta_{23} < 45^\circ$ case, consistent with the numerical calculations done in section 3.2. If $\theta_{23} > 45^\circ$ is supported by the future experimental data, then the lower bounds of $|\langle m \rangle_{\mu\mu}|$ and $|\langle m \rangle_{\tau\tau}|$ in Eq. (54) should be exchanged.

Case (D): the lightest neutrino mass m_3 satisfies $m_3^2 \gg |\Delta m_{32}^2|$. This case also corresponds to a nearly degenerate mass hierarchy: $m_1 \simeq m_2$ and $m_3 \simeq m_1 + \Delta m_{32}^2/(2m_1)$, where $\Delta m_{32}^2 < 0$. The approximate expressions of $\langle m \rangle_{\alpha\beta}$ can similarly be obtained as in Eq. (53) by replacing Δm_{31}^2 with Δm_{32}^2 . Then we arrive at

$$\begin{aligned}
m_1 \cos 2\theta_{12} &\lesssim |\langle m \rangle_{ee}| \lesssim m_1 , \\
0 &\lesssim |\langle m \rangle_{\mu\mu}| \lesssim m_1 , \\
m_1 \cos 2\theta_{23} + \frac{\Delta m_{32}^2}{2m_1} c_{23}^2 &\lesssim |\langle m \rangle_{\tau\tau}| \lesssim m_1 , \\
0 &\lesssim |\langle m \rangle_{e\mu}| \lesssim m_1 \sin 2\theta_{12} c_{23} , \\
0 &\lesssim |\langle m \rangle_{e\tau}| \lesssim m_1 \sin 2\theta_{12} s_{23} , \\
0 &\lesssim |\langle m \rangle_{\mu\tau}| \lesssim m_1 \sin 2\theta_{23} .
\end{aligned} \tag{55}$$

It is worth pointing out that the lower bound of $|\langle m \rangle_{\alpha\beta}|$ given in Eq. (51) or Eq. (52) should be zero if θ_{23} is finally found to lie in the second quadrant and makes $m_1 \cos 2\theta_{23} + \Delta m_{31}^2 c_{23}^2/(2m_1)$ or $m_1 \cos 2\theta_{23} + \Delta m_{32}^2 c_{23}^2/(2m_1)$ negative.

References

- [1] E. Majorana, *Nuovo Cimento* **14**, 171 (1937).
- [2] S.M. Bilenky, J. Hosek, and S.T. Petcov, *Phys. Lett. B* **94**, 495 (1980); J. Schechter and J.W.F. Valle, *Phys. Rev. D* **22**, 2227 (1980); M. Doi, T. Kotani, H. Nishiura, K. Okuda, and E. Takasugi, *Phys. Lett. B* **102**, 323 (1981); J. Bernabeu and P. Pascual, *Nucl. Phys. B* **228**, 21 (1983).
- [3] Z. Maki, M. Nakagawa, and S. Sakata, *Prog. Theor. Phys.* **28**, 870 (1962); B. Pontecorvo, *Sov. Phys. JETP* **26**, 984 (1968).
- [4] J. Beringer *et al.* (Particle Data Group), *Phys. Rev. D* **86**, 010001 (2012).
- [5] C. Jarlskog, *Phys. Rev. Lett.* **55**, 1039 (1985); D.D. Wu, *Phys. Rev. D* **33**, 860 (1986).
- [6] Z.Z. Xing, *Phys. Rev. D* **87**, 053019 (2013).
- [7] W. Konetschny and W. Kummer, *Phys. Lett. B* **70**, 433 (1977); M. Magg and C. Wetterich, *Phys. Lett. B* **94**, 61 (1980); J. Schechter and J.W.F. Valle, *Phys. Rev. D* **22**, 2227 (1980); T.P. Cheng and L.F. Li, *Phys. Rev. D* **22**, 2860 (1980); G. Lazarides, Q. Shafi, and C. Wetterich, *Nucl. Phys. B* **181**, 287 (1981); R.N. Mohapatra and G. Senjanovic, *Phys. Rev. D* **23**, 165 (1981).
- [8] For a recent review with extensive references, see: W. Rodejohann, *Int. J. Mod. Phys. E* **20**, 1833 (2011).
- [9] M. Fukugita and T. Yanagida, *Phys. Lett. B* **174**, 45 (1986).
- [10] F.P. An *et al.* (Daya Bay Collaboration), *Phys. Rev. Lett.* **108**, 171803 (2012); *Chin. Phys. C* **37**, 011001 (2013).
- [11] J.K. Ahn *et al.* (RENO Collaboration), *Phys. Rev. Lett.* **108**, 191802 (2012).
- [12] J. Bahcall and H. Primakoff, *Phys. Rev. D* **18**, 3463 (1978); L.N. Chang and N.P. Chang, *Phys. Rev. Lett.* **45**, 1540 (1980); J. Schechter and J.W.F. Valle, *Phys. Rev. D* **23**, 1666 (1981); L.F. Li and F. Wilczek, *Phys. Rev. D* **25**, 143 (1982); J. Bernabeu and P. Pascual, *Nucl. Phys. B* **228**, 21 (1983); J.D. Vergados, *Phys. Rept.* **133**, 1 (1986); P. Langacker and J. Wang, *Phys. Rev. D* **58**, 093004 (1998); A. de Gouvea, B. Kayser, and R.N. Mohapatra, *Phys. Rev. D* **67**, 053004 (2003); D. Delepine, V.G. Macias, S. Khalil, and G.L. Castro, *Phys. Lett. B* **693**, 438 (2010).
- [13] See, e.g., H. Minakata and S. Uchinami, *New J. Phys.* **8**, 143 (2006); H. Minakata, H. Nunokawa, S.J. Parke, and R. Zukanovich Funchal, *Phys. Rev. D* **76**, 053004 (2007); S.M. Bilenky, F. von Feilitzsch, and W. Potzel, *Phys. Part. Nucl.* **38**, 117 (2007); *J. Phys. G* **35**, 095003 (2008); *J. Phys. G* **36**, 078002 (2009); E. Akhmedov, J. Kopp, and M. Linder, *JHEP* **0805**, 005 (2008); *J. Phys. G* **36**, 078001 (2009); J. Kopp, *JHEP* **0906**, 049 (2009).
- [14] See, e.g., Z.Z. Xing, *Phys. Rev. D* **88**, 017301 (2013); and references therein.
- [15] G.L. Fogli, E. Lisi, A. Marrone, D. Montanino, A. Palazzo, and A.M. Rotunno, *Phys. Rev. D* **86**, 013012 (2012); D.V. Forero, M. Tortola, and J.W.F. Valle, *Phys. Rev. D* **86**, 073012 (2012); M.C. Gonzalez-Garcia, M. Maltoni, J. Salvado, and T. Schwetz, *JHEP* **1212**, 123 (2012).

- [16] N. Cabibbo, Phys. Lett. B **72**, 333 (1978).
- [17] Z.Z. Xing, Phys. Lett. B **633**, 550 (2006); Z.Z. Xing and H. Zhang, Commun. Theor. Phys. **48**, 525 (2007).
- [18] E. Komatsu *et al.* (WMAP Collaboration), Astrophys. J. Suppl. **192**, 18 (2011).
- [19] P.A.R. Ade *et al.* (Planck Collaboration), arXiv:1303.5076.
- [20] Z.Z. Xing, Phys. Rev. D **68**, 053002 (2003); Y.F. Li and S.S. Liu, Phys. Lett. B **706**, 406 (2012).
- [21] See, e.g., M. Frigerio and A.Yu. Smirnov, Phys. Rev. D **67**, 013007 (2003); Z.Z. Xing, Phys. Rev. D **69**, 013006 (2004); A. Merle and W. Rodejohann, Phys. Rev. D **73**, 073012 (2006); S. Zhou and J.Y. Liu, Phys. Rev. D **87**, 093010 (2013).
- [22] See, e.g., Z.Z. Xing and S. Zhou, *Neutrinos in Particle Physics, Astronomy and Cosmology* (Zhejiang University Press and Springer-Verlag, 2011).
- [23] See, e.g., J. Garayoa and T. Schwetz, JHEP **0803**, 009 (2008); M. Kadastik, M. Raidal, and L. Rebane, Phys. Rev. D **77**, 115023 (2008); A.G. Akeroyd, M. Aoki, and H. Sugiyama, Phys. Rev. D **77**, 075010; Z.Z. Xing, Phys. Rev. D **78**, 011301 (2008); P. Fileviez Perez, T. Han, G.Y. Huang, T. Li, and K. Wang, Phys. Rev. D **78**, 015018 (2008); F. del Aguila and J.A. Aguilar-Saavedra, Nucl. Phys. B **813**, 22 (2009).
- [24] P. Ren and Z.Z. Xing, Phys. Lett. B **666**, 48 (2008); Chin. Phys. C **34**, 433 (2010).
- [25] For a recent review with extensive references, see: C. Giunti and A. Studenikin, Phys. Atom. Nucl. **72**, 2089 (2009); and references therein.
- [26] J. Schechter and J.W.F. Valle, Phys. Rev. D **22**, 2227 (1980).
- [27] W. Rodejohann and J.W.F. Valle, Phys. Rev. D **84**, 073011 (2011).
- [28] Z.Z. Xing, Phys. Lett. B **660**, 515 (2008); Phys. Rev. D **85**, 013008 (2012).
- [29] J. Schechter and J.W.F. Valle, Phys. Rev. D **25**, 2951 (1982).
- [30] M. Duerr, M. Lindner, and A. Merle, JHEP **1106**, 091 (2011).
- [31] See, e.g., Z.Z. Xing, Phys. Lett. B **530**, 159 (2002); Phys. Lett. B **539**, 85 (2002); P.H. Frampton, S.L. Glashow, and D. Marfatia, Phys. Lett. B **536**, 79 (2002); W.L. Guo and Z.Z. Xing, Phys. Rev. D **67**, 053002 (2003); H. Fritzsch, Z.Z. Xing, and S. Zhou, JHEP **1109**, 083 (2011); T. Araki, J. Heeck, and J. Kubo, JHEP **1207**, 083 (2012).